Cite as: D. Niu *et al.*, *Science* 10.1126/science.aan4187 (2017).

Inactivation of porcine endogenous retrovirus in pigs using CRISPR-Cas9

Dong Niu,[1,2*] Hong-Jiang Wei,[3,4*] Lin Lin,[5*] Haydy George,[1*] Tao Wang,[1*] I-Hsiu Lee,[1*] Hong-Ye Zhao,[3] Yong Wang,[6] Yinan Kan,[1] Ellen Shrock,[7] Emal Lesha,[1] Gang Wang,[1] Yonglun Luo,[5] Yubo Qing,[3,4] Deling Jiao,[3,4] Heng Zhao,[3,4] Xiaoyang Zhou,[6] Shouqi Wang,[8] Hong Wei,[6] Marc Güell,[1†] George M. Church,[1,7,9†] Luhan Yang[1†‡]

[1]eGenesis, Inc., Cambridge, MA 02139, USA. [2]College of Animal Sciences, Zhejiang University, Hangzhou 310058, China. [3]State Key Laboratory for Conservation and Utilization of Bio-Resources in Yunnan, Yunnan Agricultural University, Kunming 650201, China. [4]College of Animal Science and Technology, Yunnan Agricultural University, Kunming, 650201, China. [5]Department of Biomedicine, Aarhus University, 8000 Aarhus C, Denmark. [6]Department of Laboratory Animal Science, College of Basic Medical Sciences, Third Military Medical University, Chongqing, 400038, P. R. China. [7]Department of Genetics, Harvard Medical School, Boston, MA 02115, USA. [8]Research Institute of Shenzhen Jinxinnong Technology CO., LTD., Shenzhen 518106, China. [9]Wyss Institute for Biologically Inspired Engineering, Harvard University, Cambridge, MA 02138, USA.

*These authors contributed equally to this work.

†These authors contributed equally to this work.

‡Corresponding author. Email: luhan.yang@egenesisbio.com

Xenotransplantation is a promising strategy to alleviate the shortage of organs for human transplantation. In addition to the concern on pig-to-human immunological compatibility, the risk of cross-species transmission of porcine endogenous retroviruses (PERVs) has impeded the clinical application of this approach. Earlier, we demonstrated the feasibility of inactivating PERV activity in an immortalized pig cell line. Here, we confirmed that PERVs infect human cells, and observed the horizontal transfer of PERVs among human cells. Using CRISPR-Cas9, we inactivated all the PERVs in a porcine primary cell line and generated PERV-inactivated pigs via somatic cell nuclear transfer. Our study highlighted the value of PERV inactivation to prevent cross-species viral transmission and demonstrated the successful production of PERV-inactivated animals to address the safety concern in clinical xenotransplantation.

The shortage of human organs and tissues for transplantation represents one of the most significant unmet medical needs (*1*). Xenotransplantation holds great promise. Porcine organs are considered favorable resources for xenotransplantation since they are similar to human organs in size and function, and can be bred in large numbers (*2*).

However, the clinical use of porcine organs has been hindered by immunological incompatibilities (*2*) and by the potential risk of PERV transmission (*3*). PERVs are gamma retroviruses found in the genome of all pig strains and can be vertically transferred through inheritance (*4*). Although to date, no study has shown PERV transmission to humans in clinical settings, it has been demonstrated that PERVs can infect human cells (*3*, *5*) and integrate into human genome in cell culture (*6*). PERV integration could potentially lead to immunodeficiency and tumorigenesis, as reported with other retroviruses (*7*, *8*).

We recently demonstrated a method to inactivate all 62 copies of PERVs in an immortalized porcine cell line (PK15) and eliminated PERV transmission to human cells (*5*). In the present study, we adopted a strategy to conduct multiplexed genome engineering to inactivate PERV activity in a primary porcine fibroblast cell line; then we used the modified fibroblasts to produce embryos through somatic cell nuclear transfer (SCNT) and transferred the SCNT embryos into surrogate sows. Using such an approach, we successfully generated PERV-inactivated pigs.

We previously demonstrated the transmission of PERVs from an immortalized pig epithelial cell line, PK15, to GFP-labeled human embryonic kidney cells (HEK293T-GFP), after co-culturing them for one week (*5*). We wondered whether PERVs remain active and propagate in human cells. To detect this, we monitored PERV copy number both in a population and in clones of PERV-infected HEK293T-GFP cells (i-HEK293T-GFP) for more than 4 months and observed that PERV copy number increased over time (Fig. 1A and fig. S1B), as determined by droplet digital PCR (ddPCR). Consistent with previous reports (*3*, *9*), we detected that both subtypes PERV-A and PERV–B were present in the infected human cells (fig. S1B), confirming that they are human-tropic. We did not detect PERV-C in either PK15 or i-HEK293T-GFP cells (fig. S1, A and B). To determine whether the PERVs integrate into the human genome or stay episomal in the infected human cells, we performed junction capture sequencing of the infected clonal i-HEK293T-GFP cells. We detected novel PERV junctions in the human ge-

nome and observed that they are overrepresented in intragenic regions and in active chromatin areas (Fig. 1B and fig. S2, A and B).

The increased copy number of PERVs in i-HEK293T-GFP clones can be caused by intracellular transposition or by intercellular PERV transmission among human cells. To clarify this, we then examined whether infected human cells could transmit PERVs to wild-type (WT) human cells. We co-cultured clonal i-HEK293T-GFP cells with WT HEK293T cells for two weeks, and subsequently checked PERV elements in the co-cultured WT clones via PCR. We detected the robust presence of PERV elements in WT HEK293T cells with no history of contact with porcine cells (Fig. 1C and fig. S2C). The percentage of infected WT HEK293T cells varies from 20% to 97% (Fig. 1D) depending on different parental i-HEK293T-GFP clones in the co-culture. We concluded from our observations that infected human cells can transmit PERVs to previously unexposed human cells.

Generating PERV-inactivated pigs involves construction of primary porcine cells devoid of PERV activity, which can be cloned via SCNT to produce porcine embryos. We tested whether we could use the same strategy we used previously in PK15 (*5*) to inactivate the PERV activities in a primary porcine fetal fibroblast cell line (denoted as FFF3 hereafter). We first aimed to map and characterize the PERVs present in the FFF3 genome. We detected 25 copies of functional PERVs, as determined by ddPCR on the reverse transcriptase (*pol*) gene (fig. S3). The detected PERV copy number was close to the sum of 10 copies of the PERV-A *env* gene, 14 copies of the PERV-B *env* gene, and 0 copies of the PERV-C *env* gene that we identified in the genome (fig. S3) by ddPCR. Using whole genome sequencing, we further detected one additional copy of truncated PERV-B not detectable by ddPCR. We used hybridization capture followed by sequencing to map PERVs copies into the genome (Fig. 2A and fig. S4). To target these PERVs for inactivation, we designed two CRISPR guide RNAs (gRNAs) specific to the catalytic core of the PERV *pol* gene (fig. S5). After treating a population of FFF3 cells with CRISPR-Cas9 and the two gRNAs for 12 days, we observed 37% PERV *pol* inactivation. Notably, we observed a bimodal distribution of targeting efficiency among single FFF3 cells after treatment, resembling our previous results obtained with PK15 cells (*5*). About 35% single cells had high editing efficiency (>90%) and 61% single cells had low editing efficiency (<20%) (Fig. 2B). Unfortunately, despite the presence of highly modified cells in the population, we could not grow up the single-cell clones with >90% PERV editing efficiency.

We hypothesized that simultaneous DNA cleavages by Cas9 at multiple PERV sites in the FFF3 genome trigger DNA damage-induced senescence or apoptosis; hence, we could not obtain the highly modified FFF3 clones. Through screening of different anti-apoptotic strategies (figs. S6 and S7), we observed that the application of a cocktail containing p53 inhibitor, pifithrin alpha (PFTα), and basic fibroblast growth factor, bFGF, during genetic modification, significantly increased the average targeting efficiency of the resulting FFF3 populations (fig. S6A (ANOVA, $p = 0.00002$), fig. S6B). Using this optimized cocktail, we were able to grow up 100% PERV-inactivated FFF3 cells (PERV-inactivated FFF3) from the population treated with CRISPR-Cas9 (Fig. 2, C and D).

Having confirmed that we genetically mutated PERV *pol* in the genome, we performed RNA-seq (fig. S8) on PERV-inactivated FFF3 clones and confirmed that all *pol* transcripts had been mutated. Furthermore, we examined whether the genome-wide disruption of PERV *pol* would eliminate in vitro production of PERVs from FFF3. We could not detect reverse transcriptase (RT) activity of PERVs in the cell culture supernatant of the PERV-inactivated FFF3 (fig. S9), suggesting that there is no viral particle secreted by the modified cells.

We next sought to examine off-target effects of CRISPR-Cas9 in the PERV-inactivated FFF3. We carried out karyotyping of 8 PERV-inactivated FFF3 and observed that 5 carried chromosomal abnormalities. Of note, the translocation sites in the genome tend to correlate with presence of PERV cutting sites, suggesting that CRISPR-Cas9 on-target toxicity may contribute to the translocations observed (fig. S10A). The remaining 3 PERV-inactivated FFF3 clones carry normal chromosomal structures (fig. S10B). To examine chromosomal integrity with higher resolution, we performed PERV genomic junctions sequencing on the 3 normal karyotype clones to examine potential deletions between Cas9-induced double-strand breaks (DSBs). All 21 tested junctions remained intact (fig. S11), which indicates no Cas9-induced macrodeletions in these regions. Therefore, we concluded that we could obtain PERV-inactivated FFF3 without detectable structural variations.

Having obtained PERV-inactivated FFF3 cells, we attempted to produce PERV-inactivated embryos via SCNT. For every round of embryogenesis, ~20-40% of the constructed PERV-inactivated embryos reached blastocyst stage after being cultured for 6 days (Methods), which is within the normal range of porcine SCNT efficiency. We observed normal 64-cell stage blastocyst structure and validated the pluripotency of inner cell mass (detected by SOX2 antibody) on day 6 (fig. S12A). We performed genomic deep sequencing to check the PERV *pol* genotypes in embryos, and confirmed 100% PERV-inactivation efficiency (fig. S12B).

Next, we transferred the PERV-inactivated embryos into surrogate sows which are PERV-C free and present a total PERV copy number of 12-30 (fig. S13A). We detected pregnancy rates of 75% (33/44), 63% (28/44), and 52% (23/44)

for PERV-inactivated FFF3 cells at day 23, 51 and 70, respectively, and 100% (5/5) for WT cells at all the three time points. Fetuses at pregnancy date 50 were analyzed, all PERV-inactivated fetuses showed 100% PERV inactivation (fig. S12, C and D) and similar PERV copy number as WT FFF3 (fig. S13B). Despite the lower pregnancy efficiency, which is commonly observed in transgenic pig production (*10*), we successfully produced putative PERV- inactivated pigs (Fig. 3A and fig. S14). We did not observe difference between PERV-inactivated and WT cells on the SCNT efficiency. The ratios of piglets born/number of embryos transferred are similar for PERV-inactivated cells (0.9%) and WT cells (0.8%). To test PERV inactivation in these pigs, we isolated genomic DNA from both the bulk cells and single cell clones derived from these pigs and observed that all the pigs exhibited ~100% PERV inactivation at the genomic DNA level (Fig. 3B and fig. S15, A and B). In addition, we observed that the copy number of PERVs in the generated pigs stays close to 25, reconfirming that there is no reinfection (fig. S15C). We further isolated total RNAs from a variety of tissues of the pigs and confirmed ~100% PERV inactivation at the mRNA level (Fig. 3C). We performed karyotyping and did not detect abnormal structural changes in the PERV-inactivated pigs (fig. S16). The PERV-inactivated pig production is robust that we have so far produced 37 PERV-inactivated piglets from 17 sows (200-300 embryo transferred/sow), 15 piglets remain alive, and the oldest healthy animals are 4-month old. We are conducting long term studies to monitor the impact of PERV-inactivation and gene editing on big animals.

In summary, we observed in our studies that PERVs can be transmitted from pig to human cells and transmitted among human cells in vitro. These results substantiate the risk of cross-species viral transmission in the context of xenotransplantation. To work toward eliminating this risk, we generated PERV-inactivated primary porcine cell lines using a combination of CRISPR-Cas9, apoptosis inhibitor and growth factor, and with these cell lines, we produced PERV-inactivated porcine embryos, fetuses, and live pigs.

In this study, we discovered that treatment with p53 inhibitor can mitigate the stress from multiplex DNA damage during multiplexible genome engineering and support clonal expansion of 100% PERV-inactivated cells. Although we have focused in this paper on the applications to xenotransplantation, we envision, more generally, that the synergistic combination of CRISPR-Cas technology with anti-apoptosis treatment may also be used to enable large-scale genome engineering in primary cells for a broad range of applications, including pathway engineering and modifications of other genetic repetitive elements of biological interest.

Although it is still unclear whether PERVs infect humans in vivo, our study shows that PERV-infected human cells pass the PERVs robustly to fresh human cells that have no prior-exposure to pig cells. Therefore, our data substantiates the value of PERV-inactivation for safe xenotransplantation practice. The physiological functions of endogenous retrovirus, which exists in all mammalian species, remain largely unknown. Further studies on our PERV-inactivated pigs will shed light on the endogenous retrovirus functionalities in related to the hosts. Most importantly, the PERV-inactivated pig can serve as a foundation pig strain, which can be further engineered to provide safe and effective organ and tissue resources for xenotransplantation.

REFERENCES AND NOTES

1. D. Shafran, E. Kodish, A. Tzakis, Organ shortage: The greatest challenge facing transplant medicine. *World J. Surg.* **38**, 1650–1657 (2014). doi:10.1007/s00268-014-2639-3 Medline
2. J.-Y. Deschamps, F. A. Roux, P. Saï, E. Gouin, History of xenotransplantation. *Xenotransplantation* **12**, 91–109 (2005). doi:10.1111/j.1399-3089.2004.00199.x Medline
3. C. Patience, Y. Takeuchi, R. A. Weiss, Infection of human cells by an endogenous retrovirus of pigs. *Nat. Med.* **3**, 282–286 (1997). doi:10.1038/nm0397-282 Medline
4. J. Denner, How active are porcine endogenous retroviruses (PERVs)? *Viruses* **8**, 215 (2016). doi:10.3390/v8080215 Medline
5. L. Yang, M. Güell, D. Niu, H. George, E. Lesha, D. Grishin, J. Aach, E. Shrock, W. Xu, J. Poci, R. Cortazio, R. A. Wilkinson, J. A. Fishman, G. Church, Genome-wide inactivation of porcine endogenous retroviruses (PERVs). *Science* **350**, 1101–1104 (2015). doi:10.1126/science.aad1191 Medline
6. Y. Moalic, Y. Blanchard, H. Félix, A. Jestin, Porcine endogenous retrovirus integration sites in the human genome: Features in common with those of murine leukemia virus. *J. Virol.* **80**, 10980–10988 (2006). doi:10.1128/JVI.00904-06 Medline
7. M. Bendinelli, D. Matteucci, H. Friedman, Retrovirus-induced acquired immunodeficiencies. *Adv. Cancer Res.* **45**, 125–181 (1985). doi:10.1016/S0065-230X(08)60268-7 Medline
8. L. J. Wegman-Points, M. L. T. Teoh-Fitzgerald, G. Mao, Y. Zhu, M. A. Fath, D. R. Spitz, F. E. Domann, Retroviral-infection increases tumorigenic potential of MDA-MB-231 breast carcinoma cells by expanding an aldehyde dehydrogenase (ALDH1) positive stem-cell like population. *Redox Biol.* **2**, 847–854 (2014). doi:10.1016/j.redox.2014.06.006 Medline
9. C. Patience, W. M. Switzer, Y. Takeuchi, D. J. Griffiths, M. E. Goward, W. Heneine, J. P. Stoye, R. A. Weiss, Multiple groups of novel retroviral genomes in pigs and related species. *J. Virol.* **75**, 2771–2775 (2001). doi:10.1128/JVI.75.6.2771-2775.2001 Medline
10. J. Zhao, J. Whyte, R. S. Prather, Effect of epigenetic regulation during swine embryogenesis and on cloning by nuclear transfer. *Cell Tissue Res.* **341**, 13–21 (2010). doi:10.1007/s00441-010-1000-x Medline
11. M. A. M. Groenen, A. L. Archibald, H. Uenishi, C. K. Tuggle, Y. Takeuchi, M. F. Rothschild, C. Rogel-Gaillard, C. Park, D. Milan, H.-J. Megens, S. Li, D. M. Larkin, H. Kim, L. A. F. Frantz, M. Caccamo, H. Ahn, B. L. Aken, A. Anselmo, C. Anthon, L. Auvil, B. Badaoui, C. W. Beattie, C. Bendixen, D. Berman, F. Blecha, J. Blomberg, L. Bolund, M. Bosse, S. Botti, Z. Bujie, M. Bystrom, B. Capitanu, D. Carvalho-Silva, P. Chardon, C. Chen, R. Cheng, S.-H. Choi, W. Chow, R. C. Clark, C. Clee, R. P. M. A. Crooijmans, H. D. Dawson, P. Dehais, F. De Sapio, B. Dibbits, N. Drou, Z.-Q. Du, K. Eversole, J. Fadista, S. Fairley, T. Faraut, G. J. Faulkner, K. E. Fowler, M. Fredholm, E. Fritz, J. G. R. Gilbert, E. Giuffra, J. Gorodkin, D. K. Griffin, J. L. Harrow, A. Hayward, K. Howe, Z.-L. Hu, S. J. Humphray, T. Hunt, H. Hornshøj, J.-T. Jeon, P. Jern, M. Jones, J. Jurka, H. Kanamori, R. Kapetanovic, J. Kim, J.-H. Kim, K.-W. Kim, T.-H. Kim, G. Larson, K. Lee, K.-T. Lee, R. Leggett, H. A. Lewin, Y. Li, W. Liu, J. E. Loveland, Y. Lu, J. K. Lunney, J. Ma, O. Madsen, K. Mann, L. Matthews, S. McLaren, T. Morozumi, M. P. Murtaugh, J. Narayan, D. T. Nguyen, P. Ni, S.-J. Oh, S. Onteru, F. Panitz, E.-W. Park, H.-S. Park, G. Pascal, Y. Paudel, M. Perez-Enciso, R. Ramirez-Gonzalez, J. M. Reecy, S. Rodriguez-Zas, G. A.

Rohrer, L. Rund, Y. Sang, K. Schachtschneider, J. G. Schraiber, J. Schwartz, L. Scobie, C. Scott, S. Searle, B. Servin, B. R. Southey, G. Sperber, P. Stadler, J. V. Sweedler, H. Tafer, B. Thomsen, R. Wali, J. Wang, J. Wang, S. White, X. Xu, M. Yerle, G. Zhang, J. Zhang, J. Zhang, S. Zhao, J. Rogers, C. Churcher, L. B. Schook, Analyses of pig genomes provide insight into porcine demography and evolution. *Nature* **491**, 393–398 (2012). doi:10.1038/nature11622 Medline

12. M. Güell, L. Yang, G. M. Church, Genome editing assessment using CRISPR Genome Analyzer (CRISPR-GA). *Bioinformatics* **30**, 2968–2970 (2014). doi:10.1093/bioinformatics/btu427 Medline
13. J. Zhang, K. Kobert, T. Flouri, A. Stamatakis, PEAR: A fast and accurate Illumina Paired-End reAd mergeR. *Bioinformatics* **30**, 614–620 (2014). doi:10.1093/bioinformatics/btt593 Medline
14. R. Tomii, M. Kurome, N. Wako, T. Ochiai, H. Matsunari, K. Kano, H. Nagashima, Production of cloned pigs by nuclear transfer of preadipocytes following cell cycle synchronization by differentiation induction. *J. Reprod. Dev.* **55**, 121–127 (2009). doi:10.1262/jrd.20126 Medline
15. H. Wei, Y. Qing, W. Pan, H. Zhao, H. Li, W. Cheng, L. Zhao, C. Xu, H. Li, S. Li, L. Ye, T. Wei, X. Li, G. Fu, W. Li, J. Xin, Y. Zeng, Comparison of the efficiency of Banna miniature inbred pig somatic cell nuclear transfer among different donor cells. *PLOS ONE* **8**, e57728 (2013). doi:10.1371/journal.pone.0057728 Medline

ACKNOWLEDGMENTS

We thank J. Markmann from Massachusetts General Hospital and P. O'Connell from Sydney University for providing advices on xenotransplantation; J. Hu from the Alt lab at Boston Children's' Hospital for assistance with junction capture sequencing; Y. Takeuchi from University College London for his insightful comments on virus interference; T. Ferrante from WYSS Institute, Harvard University for his assistance with embryo imaging and members of the Seidman lab at Harvard Medical School for advice regarding ddPCR. This study is mainly funded by eGenesis Inc. and was funded by NIH grant P50 HG005550. Y.L. was funded by Danish Research Council for Independent Research (DFF-1337-00128) and Sapere Aude Young Research Talent Prize (DFF-1335-00763). M.G. was funded by a Human Frontiers Science Program Long Term fellowship. Some of the pig production was funded by Major Program on Basic Research Projects of Yunnan Province, China (Grant No. 2014FC006). PERV elements genotyping Illumina MiSeq data have been uploaded to the European Nucleotide Archive (ENA) hosted by the European Bioinformatics Institute (EBI) with the submission reference PRJEB11222. LY is the CSO and board member of eGenesis. GC is the co-founder and scientific advisor of eGenesis. LY is the inventor on provisional patent applications #62/487,898 and #62/527,702 that are submitted by eGenesis and cover PERV-inactivated pig production.

SUPPLEMENTARY MATERIALS

www.sciencemag.org/cgi/content/full/science.aan4187/DC1
Materials and Methods
Figs. S1 to S16
Table S1
References (*12–15*)

10 April 2017; accepted 3 August 2017
Published online 10 August 2017
10.1126/science.aan4187

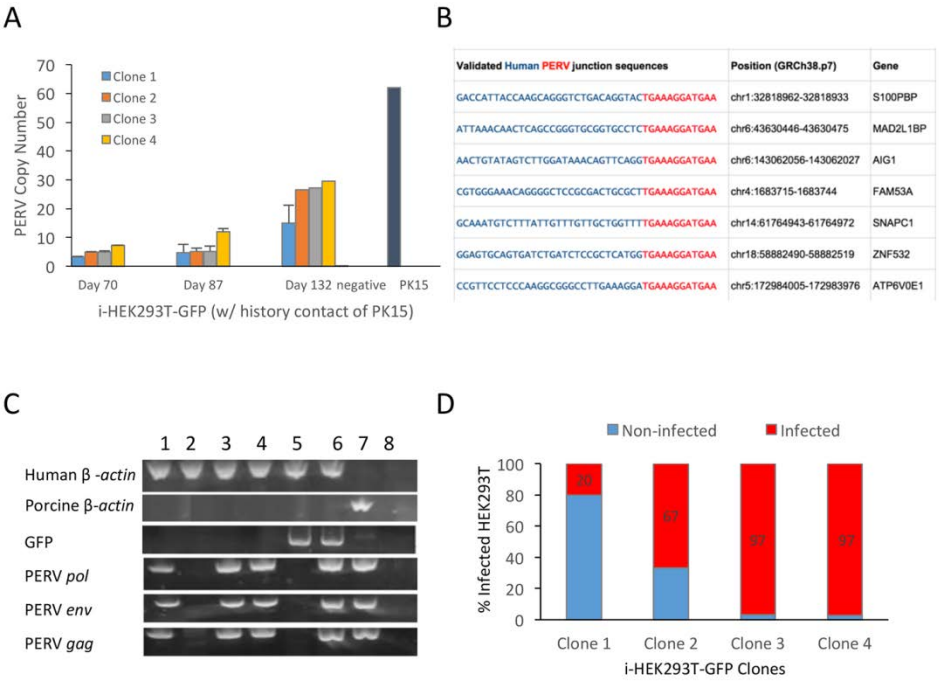

Fig. 1. Pig-to-human and human-to-human PERVs transmission. (**A**) PERVs copy number in infected human cells increases over time when co-cultured with PK15 cells. Human HEK293T-GFP cells were co-cultured with equivalent numbers of pig PK15 cells for one week. HEK293T-GFP without any contact of PK15 cells were used as negative control (negative). (**B**) Detection of PERVs insertion sites in human genome. Among the 22 PERV insertion sites detected by inverse PCR, 15 were mapped to the intragenic region. We tested a portion of the intragenic hits and validated 7 out of 12 by junction PCR (shown here). The 30bp human genomic sequences are shown in blue, whereas the PERV LTRs are shown in red. (**C**) Detection of human-to-human PERVs transmission. Individual clones of HEK293T were grown from the single cells isolated from the co-culture of i-HEK293T-GFP with HEK293T through flow cytometry. The PCR gel image showed that 3 out of 4 randomly tested HEK293T clones were infected, which contained PERVs sequences (PERV *pol*, *env*, and *gag*), but no sequence of GFP or pig genomic DNA (tested by pig specific GGTA). Sample orders are: 1) HEK293T clone 1; 2) HEK293T clone 2; 3) HEK293T clone 3; 4) HEK293T clone 4; 5) HEK293T-GFP control; 6) i-HEK293T-GFP; 7) PK15 WT; and 8) negative. (**D**) Four different i-HEK293T-GFP clones have different infectious potential. Four infected parental i-HEK293T-GFP clones are co-cultured with WT HEK293T. The PERV copy number of the 4 parental i-HEK293T-GFP clones are 15, 28, 27 and 28, respectively. The percentages of the infected WT HEK293T clones from the co-culture of i-HEK293T-GFP and WT HEK293T varied from 20% to 97%. Primers used are listed in the table S1.

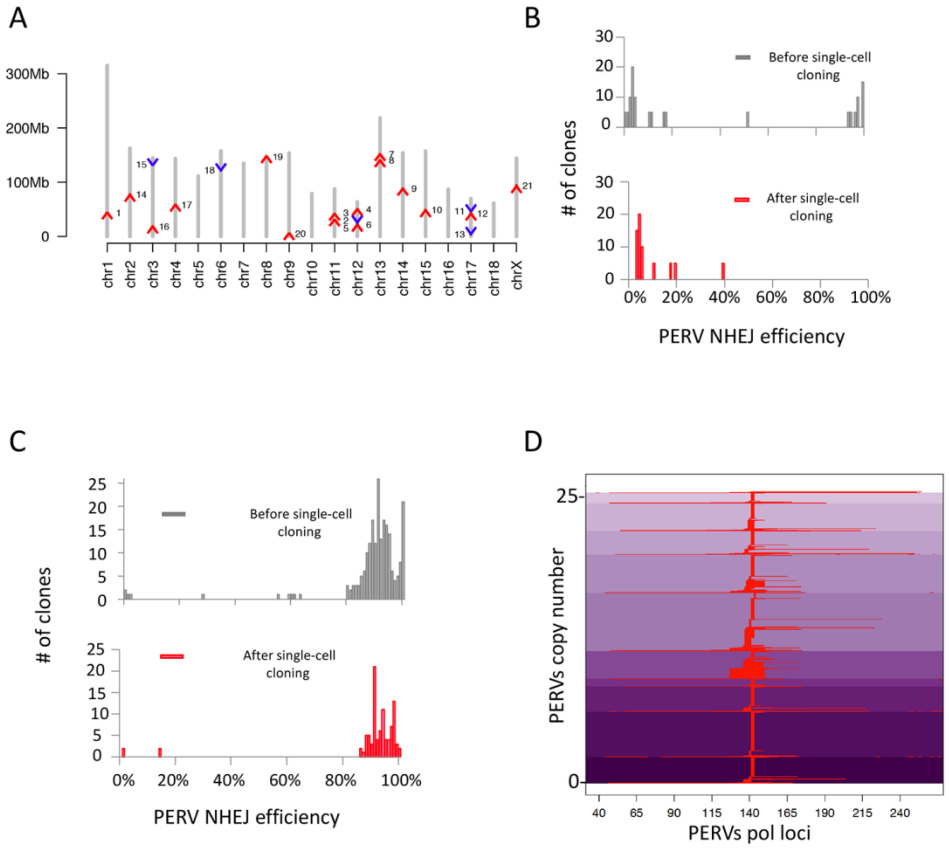

Fig. 2. PERVs insertion sites mapping, and genome-wide inactivation. (**A**) Chromosome mapping of PERVs locations in FFF3. Chromosomal scaffolds are in gray. Red arrows represent PERVs in the forward or positive chain of chromosome. Blue arrows represent PERVs in the reverse or negative chain. Y-axis represents chromosomal coordinates. Two additional copies were mapped to repetitive regions, and two could not be mapped to the current pig genome assembly and are not shown (11% gaps, *Sus scrofa* build 10.2) (*11*). (**B**) Failure to obtain 100% PERV-inactivated FFF3 clones using CRISPR-Cas9. After targeting the PERVs in FFF3, single cells were sorted and immediately genotyped. We observed a bimodal distribution of PERV targeting frequencies among single cells (upper panel), similar to that seen in the PK15 clones (*5*). 100% PERV-inactivated FFF3 cells were present among the single cells directly genotyped. However, this pattern changed after expansion of the single cells (bottom panel). Among the single cell clones, we only obtained the ones with lower efficiency (≤39%, the average targeting efficiency in the population was 37%), but not the ones with 100% PERV inactivation (lower panel). (**C**) Treatment with PFTα and bFGF sustained the growth of highly modified FFF3 clones. The combined use of a p53 inhibitor, PFTα, and a growth factor, bFGF, rescued the highly modified cells. A population of FFF3 was treated with PFTα and bFGF during the gene editing experiment (Methods); then, single cells were sorted for direct genotyping and for colony growth followed by genotyping. Both the single cells and expanded clones showed similar distribution in PERV targeting efficiency, and highly modified clones survived under this condition. (**D**) Genotype of 100% PERV inactivated clones. Several 100% PERV-inactivated clones were achieved from the PFTα and bFGF treated FFF3 population. The figure shows haplotypes of one of the 100% PERV-inactivated clones at PERV *pol* loci, after CRISPR-Cas9 treatment. The y-axis indicates the edited PERVs loci. The x-axis indicates the relative locations of the indels within the PERV loci. Aligned indel events in the PERV *pol* sequence are represented in red. Shades of purple indicate different haplotypes of PERVs.

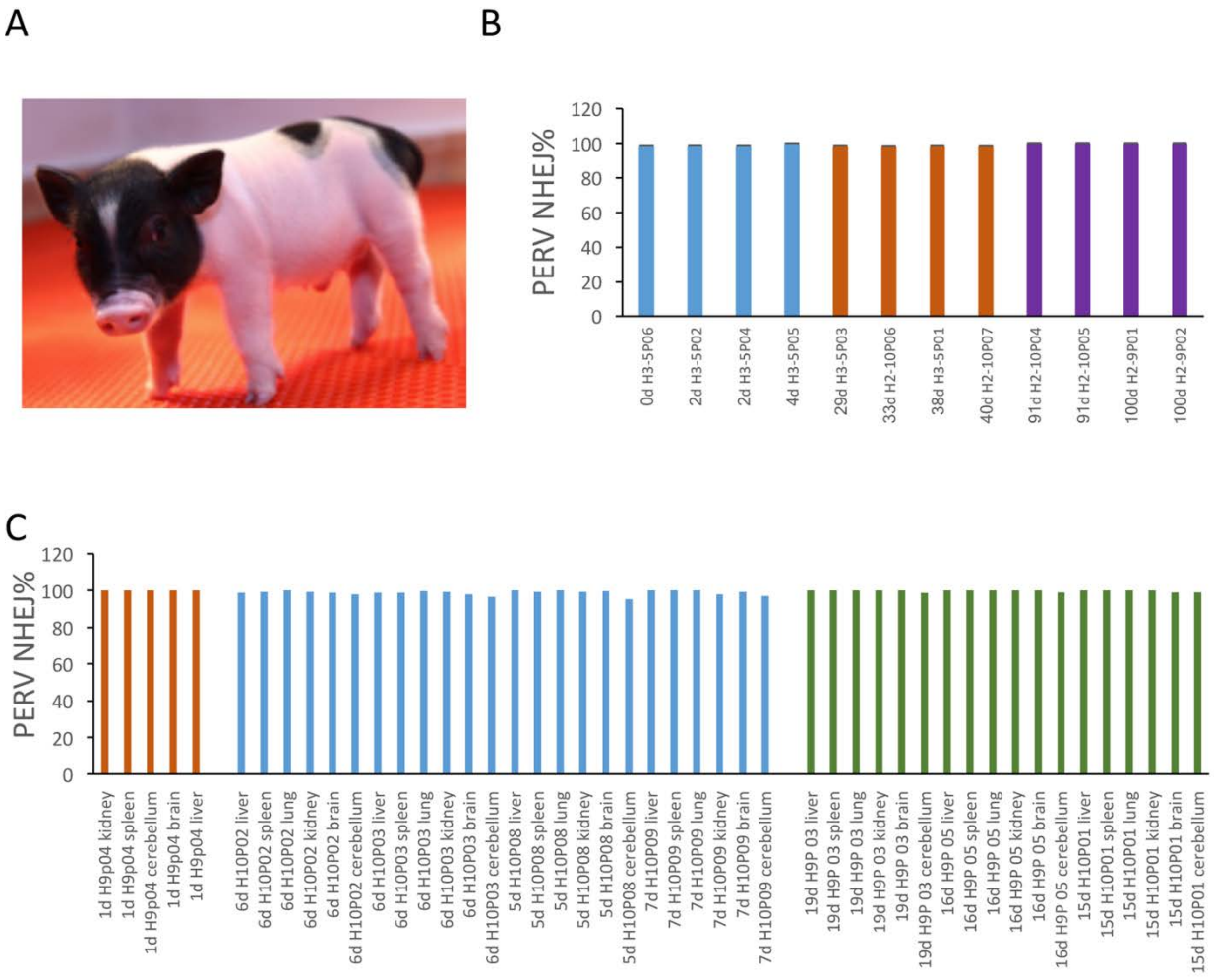

Fig. 3. PERV-inactivated pigs. (**A**) Image of the first born PERV-inactivated pig. This picture showed the first born pig (Laika) at day 2 after birth. (**B**) PERV inactivation at genomic DNA level. We genotyped PERV-inactivated pigs at different ages (up to 100 days) by deep sequencing of the PERV *pol* loci. All examined pigs showed ~100% PERV inactivation efficiency, which demonstrates that there is no detectable PERV reinfection from surrogate sows to cloned pigs. (**C**) PERV inactivation at mRNA level. Total mRNA generated cDNA was used to detect the PERV inactivation efficiency of the PERV-ko pig transcripts. All pigs exhibited ~100% PERV eradication efficiency at mRNA level.

Inactivation of porcine endogenous retrovirus in pigs using CRISPR-Cas9

Dong Niu, Hong-Jiang Wei, Lin Lin, Haydy George, Tao Wang, I-Hsiu Lee, Hong-Ye Zhao, Yong Wang, Yinan Kan, Ellen Shrock, Emal Lesha, Gang Wang, Yonglun Luo, Yubo Qing, Deling Jiao, Heng Zhao, Xiaoyang Zhou, Shouqi Wang, Hong Wei, Marc Güell, George M. Church and Luhan Yang

published online August 10, 2017

www.sciencemag.org/cgi/content/full/science.aan4187/DC1

Supplementary Materials for

Inactivation of porcine endogenous retrovirus in pigs using CRISPR-Cas9

Dong Niu,* Hong-Jiang Wei,* Lin Lin,* Haydy George,* Tao Wang,* I-Hsiu Lee,* Hong-Ye Zhao, Yong Wang, Yinan Kan, Ellen Shrock, Emal Lesha, Gang Wang, Yonglun Luo, Yubo Qing, Deling Jiao, Heng Zhao, Xiaoyang Zhou, Shouqi Wang, Hong Wei, Marc Güell,† George M. Church,† Luhan Yang†‡

*These authors contributed equally to this work.
†These authors contributed equally to this work.
‡Corresponding author. Email: luhan.yang@egenesisbio.com

Published 10 August 2017 on *Science* First Release
DOI: 10.1126/science.aan4187

This PDF file includes:

Materials and Methods

CRISPR-Cas9 gRNAs design

We used the R library DECIPHER to design specific gRNAs (sgRNA1:ggtaccctcctccagtacgtgg; sgRNA2:ggtcatccacgtactggaggagg) that target all *pol* catalytic sequences in FFF3 but not other non-PERVs retroviral sequences described before (*5*).

Cell culture

Porcine PK15 and human HEK293T cells were maintained in Dulbecco's modified Eagle's medium (DMEM, Invitrogen) high glucose with sodium pyruvate supplemented with 10% fetal bovine serum (Invitrogen), and 1% penicillin/streptomycin (Pen/Strep, Invitrogen). All cells were maintained in a humidified incubator at 37°C and 5% CO_2.

Porcine fetal fibroblast cells FFF3 were maintained in Dulbecco's modified Eagle's medium (DMEM, Invitrogen) high glucose with sodium pyruvate supplemented with 15% fetal bovine serum (Invitrogen), 1% penicillin/streptomycin (Pen/Strep, Invitrogen) and 1% HEPES (Thermo Fisher Scientific). All cells were maintained in a humidified tri-gas incubator at 38°C and 5% CO_2, 90% N_2, and 5% O_2.

PiggyBac-Cas9/2gRNAs construction and cell line establishment

Similar to the procedure previously described by Yang *et al.* (*5*), we synthesized a DNA fragment encoding U6-gRNA1-U6-gRNA2 (Genewiz) and incorporated it into a previously constructed PiggyBac-cas9 plasmid. To establish the FFF3 cell lines with PiggyBac-Cas9/2gRNAs integration, we transfected 5×10^5 FFF3 cells with 14.3 μg PiggyBac-Cas9/2gRNAs plasmid and 5.7 μg Super PiggyBac Transposase plasmid (System Biosciences) using the Neon transfection system, according to the instructions in the commercial kits (Thermo Fisher Scientific). To select the cells carrying the integrated construct, 2 μg/mL puromycin was applied to the transfected cells. Based on the negative control, in which we applied puromycin to wild type FFF3 cells, we determined that the puromycin selection was completed in 4 days. The FFF3-PiggyBac cell line was maintained with 2 μg/mL puromycin thereafter and a 2 μg/ml doxycycline was applied to induce Cas9 expression of the doxycycline-inducible FFF3-PiggyBac cell line for one week.

To avoid the Cas9-consistent expression in the FFF3 cell line, we conducted PiggyBac-Cas9/2gRNAs excision from the FFF3 genome by transfecting 5×10^5 cells with 3μg PiggyBac Excision-Only Transposase vector using Lipofectamine 2000 reagent. The PiggyBac-Cas9/2gRNAs-excised FFF3 cells were then single-cell sorted into 96-well plates for clone growth and genotyping.

Genotyping of single-cell and single cell clones

First, puromycin selection followed by PiggyBac excision was conducted on the FFF3-PiggyBac-Cas9/2gRNA cell line. Then the cells were single-cell sorted into both 96-well PCR plates for direct genotyping and 96-well cell culture plates for colony growth. To genotype single FF cells

without clonal expansion, we directly amplified the PERV loci from sorted single cells. We also conducted genotyping for the clones grown from the sorted single cells. The procedure of genotyping was according to the method of Yang *et al.* (*5*). Briefly, we sorted single cells into 96-well PCR plates with each well carrying a 5 μl lysis mixture, which contained 0.5 μl 10×KAPA express extract buffer (KAPA Biosystems), 0.1 μl of 1U/μl KAPA Express Extract Enzyme and 4.4 μl water. We incubated the lysis reaction at 75ºC for 15 min and inactivated the reaction at 95ºC for 5 min. All reactions were then added to 20μl PCR reactions containing 1× KAPA 2G fast (KAPA Biosystems), 0.2 μM PERV Illumina primers (shown as follows). Reactions were incubated at 95ºC for 3 min followed by 30 (for single cell) or 25 (for single cell clones) cycles of 95ºC, 20 s; 59ºC, 20 s and 72ºC, 10 s. To add the Illumina sequence adaptors, 3μl of reaction products were then added to 20 μl of PCR mix containing 1×KAPA 2G fast (KAPA Biosystems) and 0.3 μM primers carrying Illumina sequence adaptors. Reactions were incubated at 95ºC for 3 min, followed by 20 (for single cell) or 10 (for single cell clones) cycles of 95ºC, 20 s; 59ºC, 20 s and 72ºC, 10 s. PCR products were checked on EX 2% gels (Invitrogen), followed by the recovery of ~360 bp target products from the gel. These products were then mixed at roughly the same amount, purified (QIAquick Gel Extraction Kit), and sequenced with MiSeq Personal Sequencer (Illumina). We then analyzed deep sequencing data and determined the PERV editing efficiency using CRISPR-GA (*12*).

Primers used in the PERV *pol* genotyping

Illumina_PERV_*pol* forward:

5'-ACACTCTTTCCCTACACGACGCTCTTCCGATCTCGACTGCCCCAAGGGTTCAA-3'

Illumina_PERV_*pol* reverse:

5'-GTGACTGGAGTTCAGACGTGTGCTCTTCCGATCTTCTCTCCTGCAAATCTGGGCC-3'

PERV infectivity test of pig to human cells and human to human cells

1) PERV infectivity test of pig to human cells (PK15 WT to HEK293T-GFP)

The procedure is similar to that previously described by Yang *et al*. (*5*). Briefly, 1×105 HEK293T-GFP cells and 1×105 PK15 WT cells were co-cultured in a 10 cm dish for one week. Sequential cell sorting was conducted through flow cytometry to obtain high purity GFP positive HEK293T-GFP cells. The HEK293T-GFP cells were sorted as bulk and cultured for 125 days. Genomic DNAs were isolated from the cells at different time points (d76, d80, and d125) to detect whether the PERV copy number increased with time going via ddPCR. We also conducted single cell sorting from the bulk cells at different time points. After the single cell grew up into clones, we examined the PERV infection of some clones by PCR first and then quantified the PERV copy number of the PERV-infected clones via ddPCR.

2) PERV infectivity test of human to human cells (i-HEK293T-GFP to WT HEK293T)

To test whether the PERV can be transmitted from human to human cells, 1×10^5 PERV-infected HEK293T-GFP (i-HEK293T-GFP) cells were co-cultured with 1×10^5 WT HEK293T cells for 2 weeks, then the GFP negative single cells were sorted via flow cytometry. After the single cell grew up

into clones, we examined the PERV infection ratio of GFP negative clones which had contact with different i-HEK293T-GFP clones by PCR. Particularly, we quantified the PERV copy number of GFP negative clones which were co-cultured with i-HEK293T-GFP clone 10 via qPCR using the PERV copy number of i-HEK293T-GFP clone 10 as the standard marker (PERV copy number of clone 10 has been detected by ddPCR previous to the co-coculture experiment).

Reverse transcriptase (RT) assay

The RT assay is the same as the protocol previously described by Yang *et al*. (*5*). Briefly, to test the RT activity of the wild type FFF3 cells and 100% PERV-modified FFF3 clones, we plated 5×10^5 cells in 10 cm Petri dishes, and collected the supernatant after the cells reached 80% confluency. The media were first centrifuged at 400 g for 4 min to get rid of cells and debris, then filtered with a 0.45 µm pore size Millex-HV Syringe Filter (EMD Millipore Corporation). The filtered supernatant was concentrated at 4000g for 10min using Amicon Ultra-15 Centrifugal Filter Unit (EMD Millipore Corporation). The concentrated supernatant was then ultra-centrifuged at 50,000 rpm for 60 min. The supernatant was carefully removed, and the virus pellet was fully re-suspended and lysed with 20 µl of 10% NP40 at 37℃ for 60 min. The RT reaction was conducted using the Omniscript RT Kit (Qiagen). The total volume of the reaction was 20 µl, which contained 1× RT buffer, 0.5 mM dNTPs, 0.5 µM Influenza reverse primer (5' CTGCATGACCAGGGTTTATG 3'), 100 units of RnaseOUT (Life Technology, Invitrogen), 100 units of SuperRnase Inhibitor (Life Technologies), 5 µl of sample lysis and 40 ng of IDT-synthesized Influenza RNA template which was Rnase resistant in both 5' and 3' end. The RNA template sequence was 5'
rA*rA*rC*rA*rU*rGrGrArArCrCrUrUrUrGrGrCrCrCrUrGrUrUrCrArUrUrUrUrArGrArArArUr
CrArArGrUrCrArArGrArUrArCrGrCrArGrArArGrArGrUrArGrArCrArUrArArArCrCrCrUrGrGrUrCrAr
UrGrCrArGrA-rCrCrU*-rC*rA*rG*rU*rG 3' (* phosphodiester bond). After the RT reaction was completed, the RT product was examined by PCR using Influenza forward (5' ACCTTTGGCCCTGTTCATTT 3') and Influenza reverse primers (sequence shown as above). The expected size of the amplicon was 72 bp.

.

PERV copy number quantification

As described earlier by Yang *et al*. (*5*), we used Droplet Digital PCR™ (ddPCR™) to quantify the copy number of PERVs according to the manufacturer's instructions (BioRad). Briefly, genomic DNA was extracted (DNeasy Blood & Tissue Kit, Qiagen) from cultured cells, and 50 ng genomic DNA was digested with MseI (10U) at 37ºC for 3 hrs, followed by inactivation at 65ºC for 10 min. Then the ddPCR reaction was prepared; the reaction mixture contains 1× ddPCR Master mix, 1 µl of 18 µM target primers & 5 µM target probe (VIC), 1 µl of 18 µM reference primers & 5 µM reference probe, 5 ng digested DNA, and water to total volume of 20 µl. The sequences of the primers and the probe information can be found in Table S1.

After droplet generation with QX100 Droplet Generator, the droplets were carefully transferred into a 96-well PCR plate and proceeded to the thermal cycling, using a Biorad PCR machine as follows: 95ºC 10 min for enzyme activation, then 40 cycles of 94ºC 30 sec for denaturation and 60 ºC 1 min for annealing/extension (ramp rate 2 ºC/sec), then 98ºC 10 min for enzyme deactivation.

After the thermal cycling, the 96-well plate was placed in Biorad Droplet Reader and QunataSoft Software was used to set up the experimental design and read the experiment. Once the program was finished, the results were analyzed through gating, according to the manufacturer's instructions (BioRad).

Table S1- Primers used in ddPCR assay

Name	Sequence
pervA env ddpcr fw	5'-TTCGCCTCAGAATAGAAACTCAG-3'
pervA env ddpcr rv	5'-GTTAGGAGATGGCCTCTGTTCTT-3'
pervA env ddpcr probe	5'-/56-FAM/CCAAACCCTTATTTGGTCCTATAGCAAC/3BHQ_1/-3'
pervB env ddpcr fw	5'-GGGCAAGTACAAAGTGATGAAAC-3'
pervB env ddpcr rv	5'-ATTCCCCAGCTCATACCATTTAT-3'
pervB env ddpcr probe	5'-/56-FAM/ATAAGAGCTGCTCCCCATCAGACTTAGAT/3BHQ_1/-3'
pervC env ddpcr fw	5'-TAAATGGTATGTCTTGGGGAATG-3'
pervC env ddpcr rv	5'-AGACCGTATTTGGTCCTATAGCC-3'
pervC env ddpcr probe	5'-/56-FAM/CCTGGTTGTTTACCCGAGCCTCCA/3BHQ_1/-3'
PrimerPol1-FW	5'-CGACTGCCCCAAGGGTTCAA-3'
PrimerPol2-FW	5'-CCGACTGCCCCAAGAGTTCAA-3'
PrimerPol-RV	5'-TCTCTCCTGCAAATCTGGGCC-3'
ProbePol	5'-/56FAM/CACGTACTGGAGGAGGGTCACCTG-3'
Primerpig_GAPDH_F	5'-ccgcgatctaatgttctctttc-3'
Primerpig_GAPDH_R	5'-ttcactccgaccttcaccat-3'
Probepig_GAPDH	5'-/5HEX/cagccgcgtccctgagacac-3'

Targeting efficiency calculation

As previously described by Yang *et al*. (*5*), we built a custom pipeline to estimate the efficiency of PERV inactivation. Briefly, we amplified the *pol* gene and sequenced it *via* Illumina Next Generation Sequencing using PE250 or PE300. First, we combined the two overlapping reads using PEAR (*13*) and mapped to the reference region using BLAT. After mapping, we grouped the reads into sets containing specific combinations of haplotypes, and indel types. Read sets with representation lower than 0.5% of the total number of mapped reads were discarded.

Finally, the mapping output was parsed to call the different insertions and deletions, as described by Güell *et al*. (*12*).

PERV-human junction capture

The PERV insertion sites in the highly infected i-HEK293T-GFP clones were determined by the standard inverse PCR protocol. The genomic DNA of these clones were fragmented by Sau3AI digestion and self-ligated under low DNA concentration using T4 DNA ligase (NEB). Then the fragments containing the PERV-human junctions were amplified by PCR, using primers on the PERV LTRs shown below. The PCR products were sub-cloned using the PCR Blunt II TOPO kit (Thermo Fisher) and Sanger sequenced. Sequences immediately next to the PERV LTRs were aligned to the human genome using USCS Genome Browser. Part of the hits in human genes were validated using junction PCR and Sanger sequencing.

PERV_LTR_F: 5'-ATGCCCCCGAATTCCAGA-3'

PERV_LTR_R: 5'-GGTTAGGTTGCATTTTCATCCTT-3'

In Vitro Maturation (IVM) of Oocytes

Oocyte collection and IVM culture were performed as previously described (*13*, *14*). Porcine ovaries were collected from Hongteng slaughterhouse (Chenggong Ruide Food Co., Ltd, Kunming, Yunnan Province, China). Cumulus-oocyte complexes (COCs) were aspirated from follicles with 3-6 mm diameter. COCs with at least three layers of compacted cumulus cells were selected, and approximately 50 COCs were cultured in 200 μL IVM medium at 38.5℃ in a 5% CO_2 atmosphere (APC-30D, ASTEC, Japan) with saturated humidity for 42-44 h.

Somatic Cell Nuclear Transfer (SCNT) and Embryo Transfer

SCNT and embryo transfer were performed as previously described in our previous studies (*15*). The cultured COCs were freed of cumulus cells by treating with 0.1% (w/v) hyaluronidase. The first polar body contained in the oocytes and the adjacent cytoplasm was enucleated via gentle aspiration using a beveled pipette in TLH-PVA. Donor cells from a GTKO/hCD55/hCD59-positive fibroblast cell line were inserted into the perivitelline space of an enucleated oocyte. The reconstructed embryos were fused with a single direct current pulse of 200 V/mm for 20 μs using the Electro Cell Fusion Generator (LF201, NEPA GENE Co., Ltd., Japan) in fusion medium (0.25 M D-sorbic alcohol, 0.05mM $Mg(C_2H_3O_2)_2$, 20 mg/mL BSA and 0.5mM HEPES [acid-free]). Then, the embryos were cultured for 0.5-1 h in PZM-3 and were activated with a single pulse of 150 V/mm for 100ms in activation medium containing 0.25 M D-sorbic alcohol, 0.01mM $Ca(C_2H_3O_2)_2$, 0.05mM $Mg(C_2H_3O_2)_2$ and 0.1mg/mL BSA. The embryos were equilibrated in PZM-3 supplemented with 5μg/mL cytochalasin B for 2h at 38.5℃ in a humidified atmosphere with

5% CO_2, 5% O_2 and 90% N_2 (APM-30D, ASTEC, Japan) and then cultured in PZM-3 medium with the same culture conditions described above until embryo transfer. The SCNT embryos were surgically transferred into the oviducts of the recipients. Pregnancy was confirmed approximately 23 days after surgical transfer using an ultrasound scanner (HS-101 V, Honda Electronics Co., Ltd., Yamazuka, Japan).

Immunostaining

Day 6 porcine blastocysts were fixed and stained using the Pluripotent Stem Cell 4-Marker Immunocytochemistry Kit (Molecular Probes A24881), according to the manufacturer's instructions. However, the antibodies provided by the kit were substituted with primary goat anti-pig anti-SOX2 (sc-17320) and rabbit anti-goat IgG secondary antibodies conjugated with Alexa Fluor 647 (Invitrogen A-21446). NucBlue® Live ReadyProbes® Reagent (Molecular Probes R37605) and Phalloidin (A22282) were applied five minutes before imaging. The final concentration of antibodies used in embryo staining was 1:100 for anti-SOX2, 1:200 for rabbit anti-goat IgG, 1:40 for Phalloidin and 1:100 for NucBlue.

Confocal Microscopy

Blastocysts were transferred to wells of a micro-Insert 4 Well in μ-Dish 35 mm (Ibidi 80406) and imaged using a Leica TCS SP5 Confocal Laser Scanning Microscope with a 10× water objective. Images were cropped, segmented and contrast-enhanced, using a combination of Imaris and Fiji software.

Fetus and pig analysis

To test whether there is any reinfection of PERVs from surrogate sows to the fetuses and pigs cloned from PERV-inactivated FFF3. We collected the WT (Day 75) and PERV-ko fetuses (Day 40 and Day 50) from surrogate sows by cesarean section (c-section). For pigs cloned from FFF3, we isolated genomic DNAs and total RNAs from different tissues of cloned pigs at different time points. We then checked the PERV genotypes of both genomic DNA and RNA via deep sequencing. All the PERV-ko fetuses and pigs exhibited ~100% PERV inactivation efficiency both in the genome and in the transcripts of tissues. In addition, we detected the PERV copy number of the fetuses and pigs via ddPCR and confirmed that they have similar PERV copy number as the cell line FFF3 from which they were cloned.

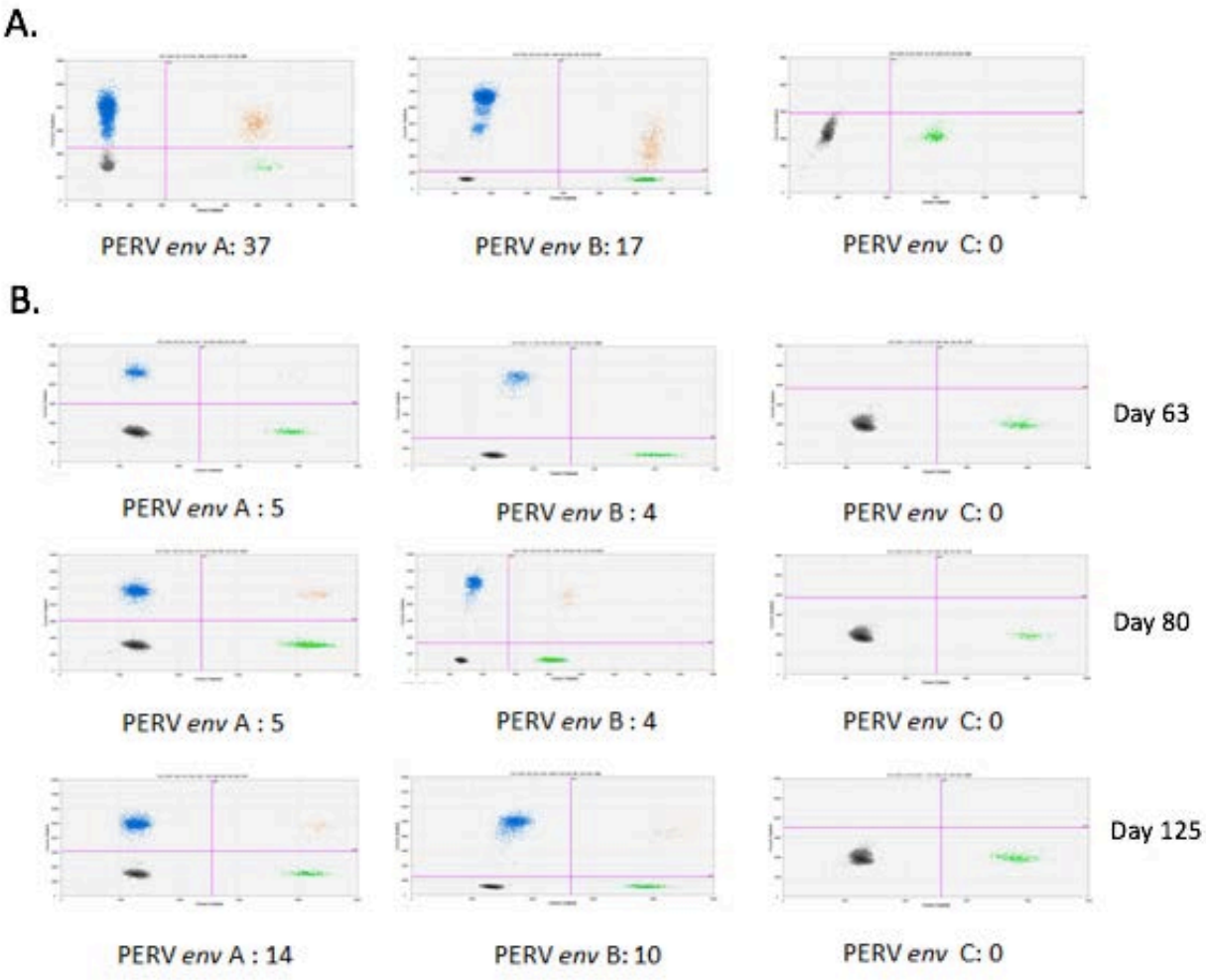

Figure S1. PERVs copy number in pig PK15 and in human HEK293T(iHEK293T-GFP) co-cultured with PK15. A) Copy number of PERV *env* A, B, C in PK15 cell line. PERV-A and PERV-B, but not PERV-C, were detected in PK15 cells. PERV-A copy number is around two times of PERV-B. In each 2D amplification plot, black dots represents droplets with no amplification, green represents droplets containing GAPDH (reference gene), blue represents droplets containing PERV *env* from subtypes A, B, or C, and orange represents droplets containing GAPDH and PERV *env*. The copy number of PERV subtypes A, B, and C, as measured relative to GAPDH, is shown under each plot. **B) PK15 transmits PERVs to HEK293T-GFP human cells, and PERV copy number in HEK293T-GFP increases over time**. HEK293T-GFP cells were co-cultured with equivalent numbers of PK15 cells. The human cell population was isolated by sequential rounds of sorting based on GFP expression. Purified human cells was collected at three time points and genomic DNA was harvested and amplified via ddPCR to detect and quantify PERV elements in the human cells. PERVs transmission from pig PK15 to human HEK293T cells was detected by ddPCR of PERV *env* gene. PERV-A and PERV-B, but not PERV-C, were detected in the HEK293T cells which have history of contact with PK15, and the PERV copy number increased in the HEK293T cells over time.

A.

Clone	Number	Chr.	Position (GRCh38.p7)	Intron/Exon	Name	Specification
7	9	1	32819140 to 32819239	intron	S100PBP	S100P binding protein
7	14	1	36528222 to 36528321			
7	25	17	8295655 to 8295757	exon	SLC25A35	Solute carrier family 25 member 35 (isoform X3/a)
7	45	2	55430992 to 55431091			
7	46	X	2578096 to 2578188			
8	24	17	56577129 to 56577184			
8	35	6	43629658 to 43629757	exon	MAD2L1BP	MAD2L1BP/MAD2L1-binding protein (isoform 1)
8	44	7	150369161 to 150369261	intron	REPIN1	Replication initiator 1 isoform 3
8	46	7	151878586 to 151878612	exon	PRKAG2-AS1	PRKAG2-AS1 according to ucsc genome browser
8	50	11	125593202 to 125593300	intron	STT3A	Dolichyl-diphosphooligosaccharide--protein glycosyltransferase
9	28	6	143062227 to 143062325	intron	AIG1	Androgen-induced gene 1 protein (isoform X4,X5/c,a)
9	34	2	130721486 to 130721587			
9	36	4	1683593 to 1683680	intron	FAM53A	Family with sequence similarity 53 member A
9	52	14	61764870 to 61764928	intron	SNAPC1	snRNA-activating protein complex subunit 1
10	12	8	80012663 to 80012710	intron	MRPS28	28S ribosomal protein S28, mitochondrial
10	25	12	92928283 to 92928348	intron	EEA1	Early endosome antigen 1
11	16	4	1744740 to 1744758	exon	TACC3	Transforming acidic coiled-coil-containing protein 3
11	43	20	30288623 to 30288660	exon	LOC107985433	Putative uncharacterized protein LOC401522
11	46	18	58882416 to 58882480	intron	ZNF532	Zinc Finger Protein 532
11	50	3	13782457 to 13782523			
11	52	14	91115855 to 91115955	intron	C14orf159	Chromosome 14 Open Reading Frame 159
11	53	5	172984252 to 172984352	intron	ATP6V0E1	V-type proton ATPase subunit e 1

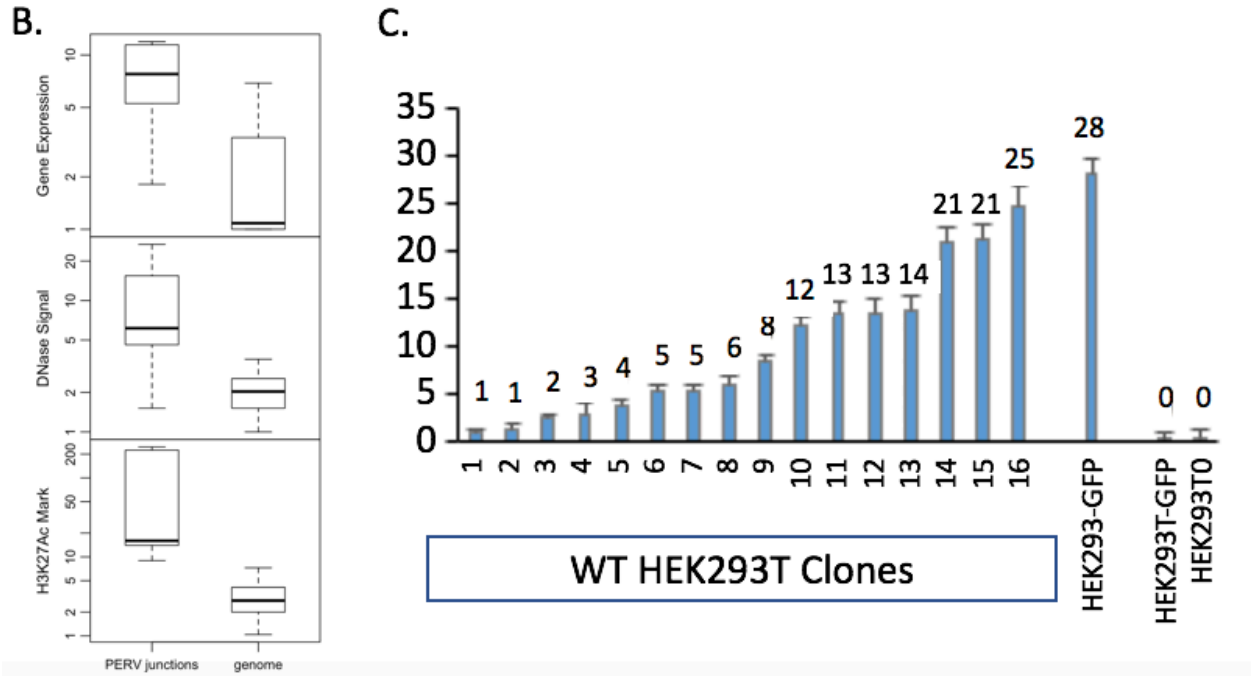

Figure S2. PERVs copy number in selected clones of iHEK293T-GFP. A) PERV-human junctions captured by inverse PCR. Part of these junctions were confirmed by junction PCR and sequencing. **B) PERVs insert preferentially in open chromatin and transcriptionally active areas**. We compared gene expression levels, Dnase signal, and H3K27Ac signals between areas around PERVs insertion sites and the whole genome. We observed increased transcription, Dnase signal, and H3K27Ac (histone acetylation) levels in PERVs insertion sites. **C) PERV transmission from PERV-infected HEK293T-GFP to WT HEK293T.** WT HEK293T (non-GFP) cells were co-cultured with equivalent number of cells of PERV infected HEK293T-GFP(i-HEK293T-GFP) clone 10 for two weeks. The GFP-negative single human cells were isolated by flow cytometry based on GFP signal. After the formation of single cell colonies, their genomic DNA was amplified via qPCR to detect and quantify PERV elements in the GFP-negative clones using

i-HEK293T-GFP clone 10 PERV copy number as standard marker (PERV copy number of clone 10 has been detected by ddPCR prior to the co-coculture experiment). PERVs transmission from i-HEK293T-GFP clone 10 to WT HEK293T human cells was detected by qPCR of PERV *pol* gene and different WT HEK293T clones showed different copy number of PERVs.

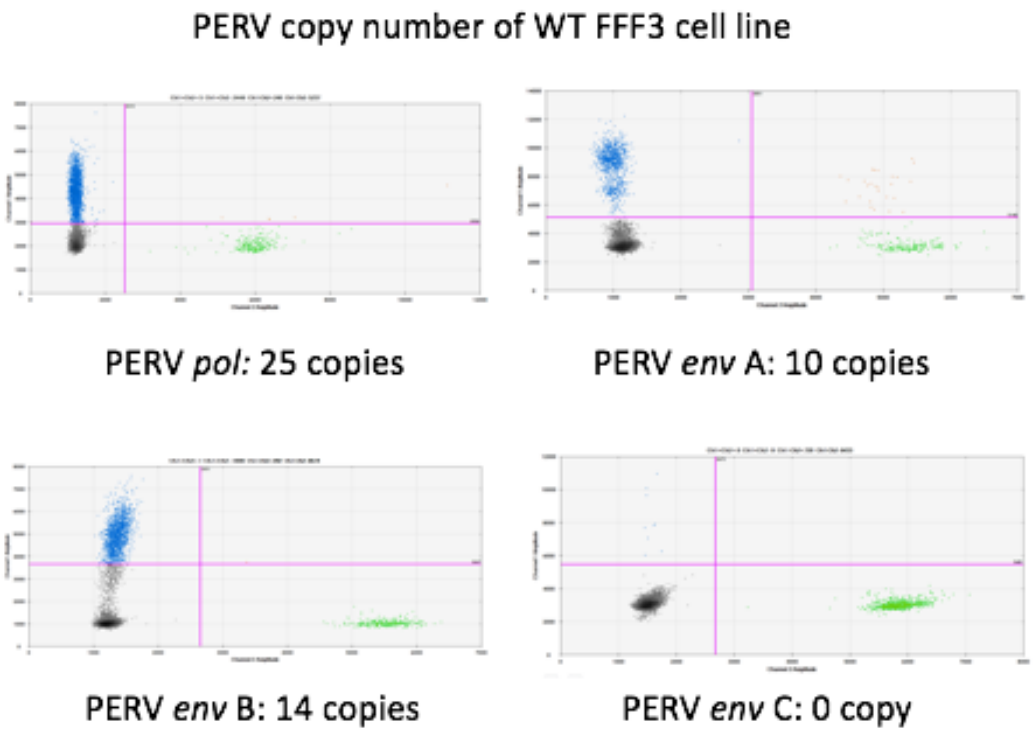

Figure S3. Validation of PERV subtype copy numbers in FFF3. PERV copy number of WT porcine primary fetal fibroblast cell line (FFF3) was detected by ddPCR of both *pol* and *env* genes. The PERV copy number (25) determined by *pol* gene is similar to that (24) detected by *env* gene.

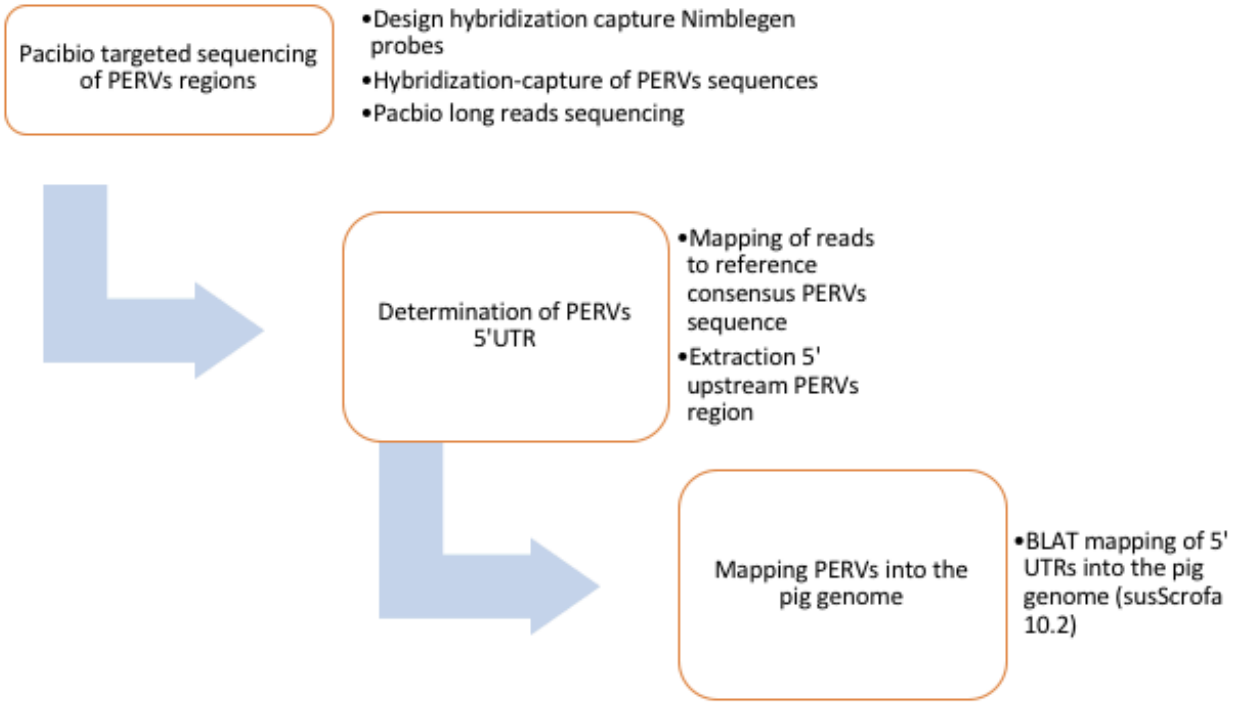

Figure S4. Determination of PERVs insertion sites. Scheme describing the process of detecting PERVs location in the pig genome. To map the locations of the PERVs, we performed PacBio long-reads genome sequencing (N50= 2,439bp, Methods) after PERVs-specific hybridization capture, and mapped 21 copies of PERVs in non-repetitive regions of the genome.

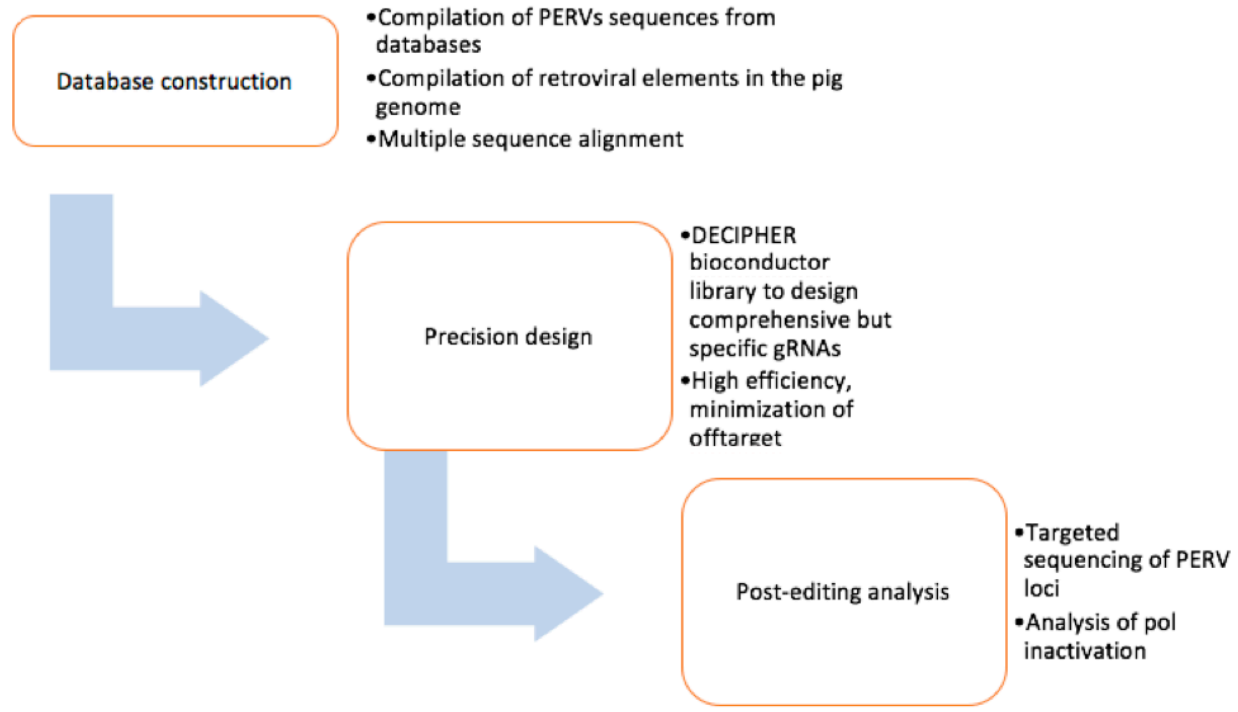

Figure S5. Scheme describing the design process of the *pol* targeting gRNAs.

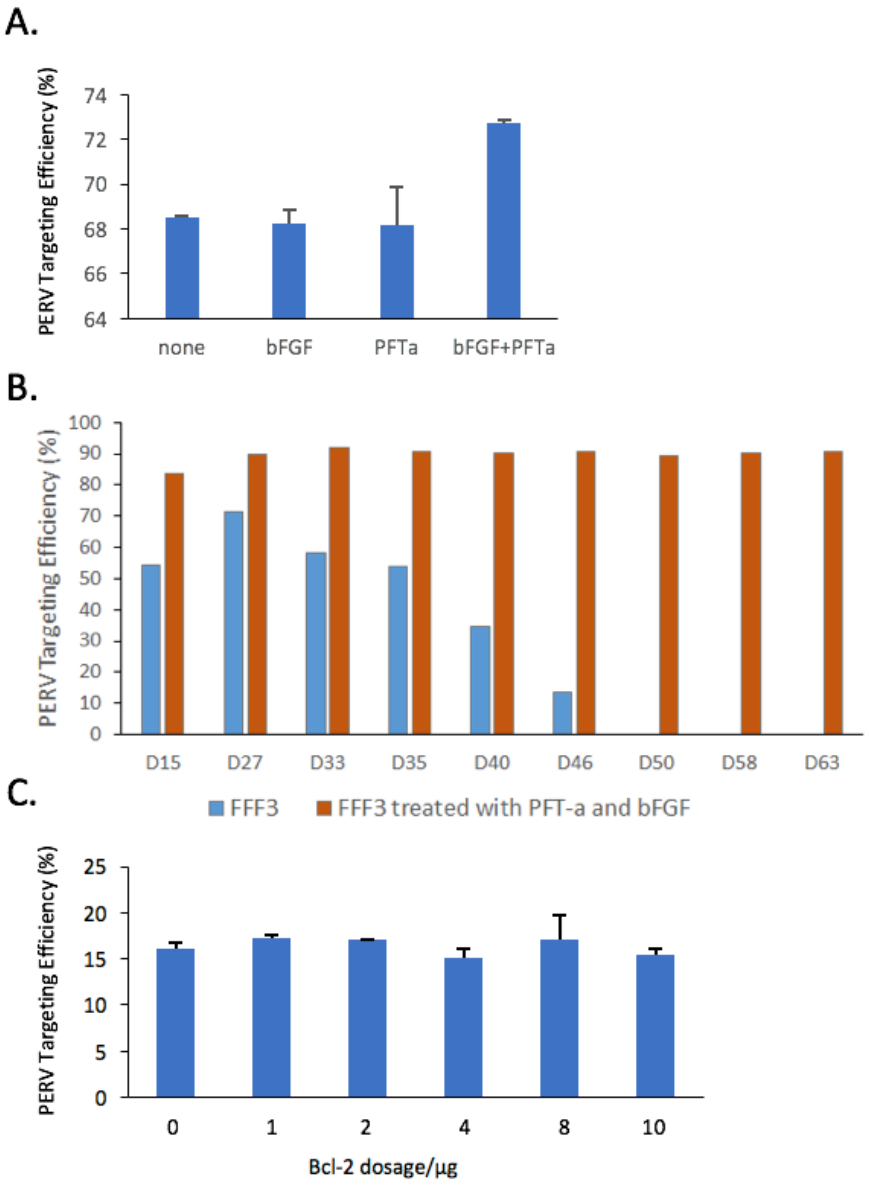

Figure S6. Effects of modulators on DNA damage repair. A) Cocktail of bFGF and PFTα increased the PERV editing efficiency. FFF3 cells were treated with bFGF, PFTα, and bFGF+PFTα. Both the bFGF and PFTα alone did not increase PERV editing efficiency, whereas cocktail of bFGF and PFTα significantly enhanced the targeting frequency (p-value=0.0016), demonstrating there exists a synergistic effect between bFGF and PFTα. **B) PFTα and bFGF cocktail rescued the PERV highly modified cells within the population.** Population of FFF3 treated with cocktail of PFTα and bFGF showed sustained high PERV targeting efficiency, whereas population of FFF3 not treated with the cocktail showed decreased pattern of PERV editing efficiency. (ANOVA, day (p-value=0.23), PFTα/bFGF treatment (p-value=0.00002)). **C) Bcl-2 treatment didn't improve the PERV editing efficiency.** Population of FFF3 was transfected with different amount of Bcl-2 plasmid and cultured for 7 days. No significant difference (p-value=0.565) among treatments with different dosages of Bcl-2 was detected. Dose-dependent cytotoxicity of Bcl-2 was observed during the experiment.

A

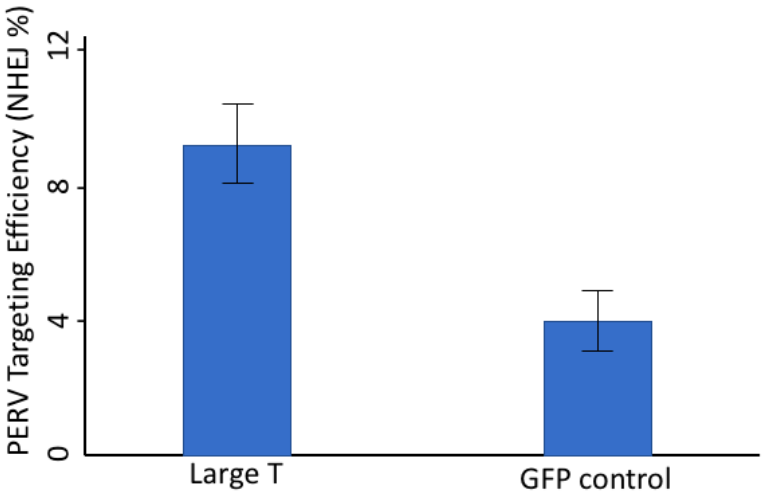

B

	>80% PERV-ko clones/total	>90% PERV-ko clones/total
No large T	2.92%	0.83%
With large T	10.94%	4.10%
Folds increased	3.75	5.06

Figure S7. Large T antigen increased PERV editing efficiency of FFF3 population. **A) Large T antigen increased the targeting efficiency of PERVs in FFF3 population** (P-value=0.05, Wilcoxon Test (One sided)). **B) Large T antigen increased the ratio of PERV highly modified clones.** Clones grown from sorted single cells were used to analyze the PERV editing efficiency of populations treated with or without large T antigen. Large T antigen treatment increased the fraction of >80% and >90% PERV-ko clones by 3.75 and 5.06 folds, respectively, compared with the untreated group. Given that it is hard to control the duration Large T antigen affect by transfecting its coding plasmid in the system, we decided to use chemical treatment as described in Figure S6 in our following experiment.

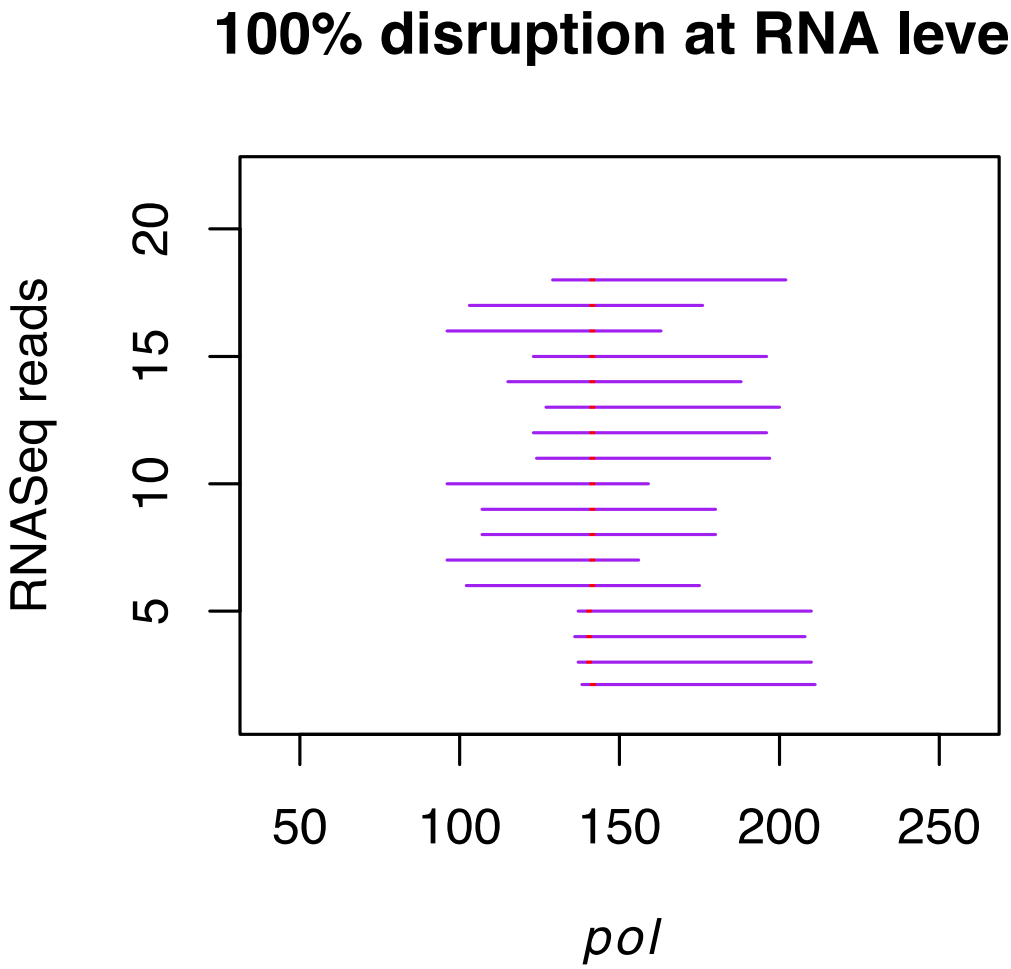

Figure S8. Transcription profile of 100% PERV-inactivated FFF3. RNAseq was used to analyze PERVs inactivation of *pol* gene. The Y-axis indicates the sites. The X-axis indicates the relative locations of the indels within the PERV loci. In purple, aligned indel events in the PERV pol sequence are represented.

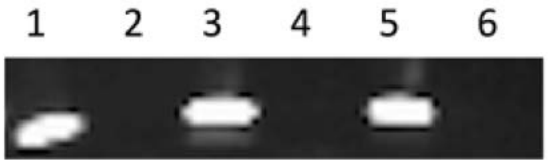

Figure S9. Elimination of PERV production in 100% PERV modified clones. The reverse transcriptase (RT) activity of PERV particles presented in the cell culture supernatant was detected by RT assay (*15*). The results demonstrated no PERV production in 100% PERV-inactivated clone supernatant, whereas the supernatant of WT FFF3 cells showed significant RT activity. The sample order from left to right: 1. RT+ (using commercial reverse transcriptase (RT)); 2. RT- (no RT enzyme); 3. RT+/FF WT (commercial RT enzyme plus WT FFF3 lysis of virus pellet from FFF3 culture media); 4. 100% PERV-ko FFF3 (100% PERV-inactivated FFF3 clone lysis); 5. WT FFF3 (WT FFF3 lysis); 6. neg (no lysis or RT enzyme, no RNA template).

A.

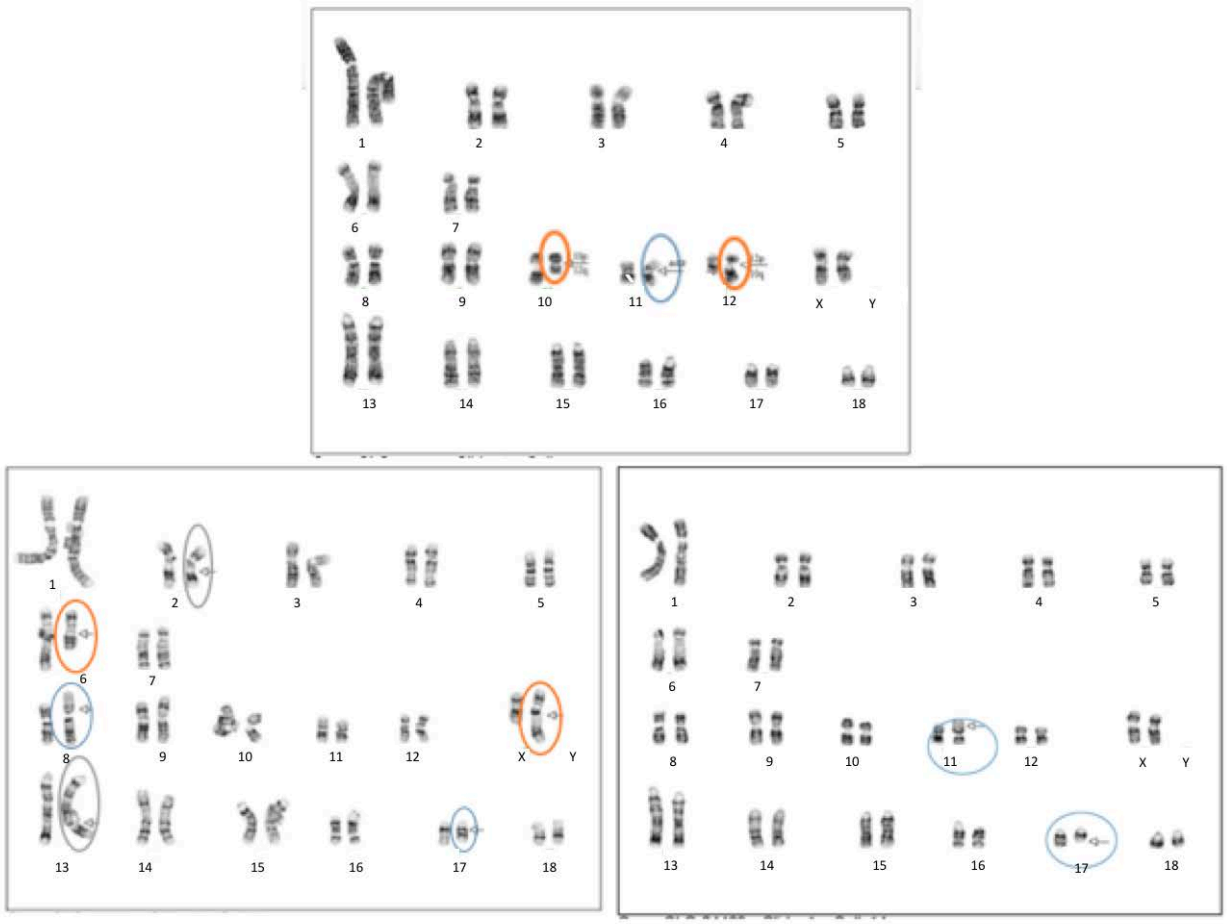

B.

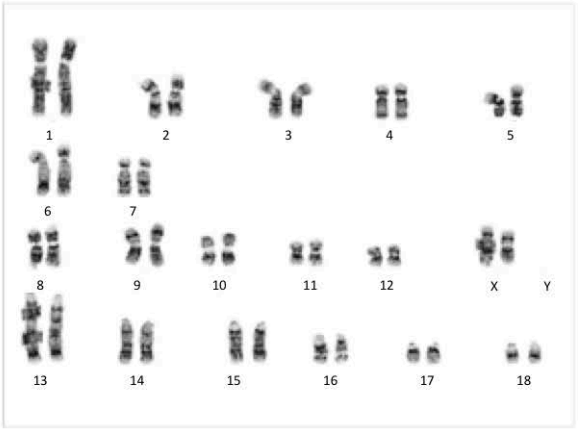

Figure S10. Karyotyping of the PERV-inactivated clones used for pig cloning. Different clones were analyzed using karyotyping, 5 showed abnormal karyotype and 3 normal. **A) Example of 3 abnormal karyotypes**. Of note, all chromosomes translocated (indicated by color pairs) or with insertion or deletions contain PERVs except in one case (chromosome 10 of the pair

translocated t(10,12), upper panel). **B) Example of normal karyotype**. This PERV-inactivated clone shows a completely normal karyotype.

A.

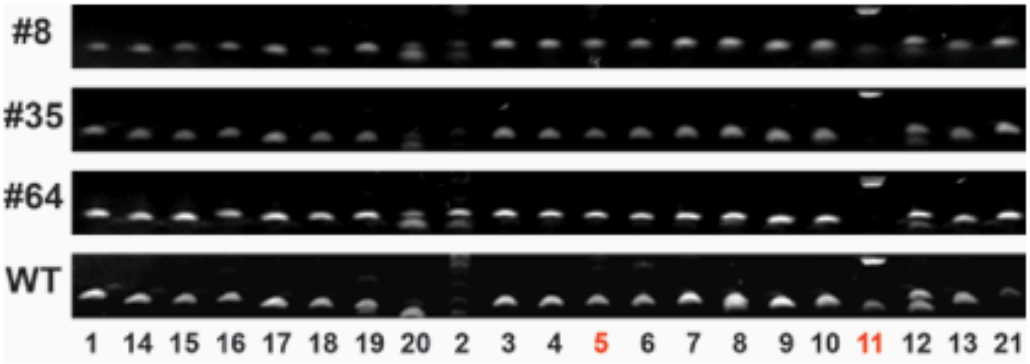

B.

PERV junction primers for FF3CF (Black: 5'LTR; Red: 3'LTR)

PERV	LTR	Forward	Reverse
1	5'	ACTCTATCCTATAAGGT	TAGGTTGCATTTTCATCCTT
14	5'	GGAGCAAAAGAGCAGT	TAGGTTGCATTTTCATCCTT
15	5'	TATATGGACGCATTCAG	TAGGTTGCATTTTCATCCTT
16	5'	TTTTCGGAGGATTTTCA	TAGGTTGCATTTTCATCCTT
17	5'	TACTGCATTTGATACCA	TAGGTTGCATTTTCATCCTT
18	5'	GACTTCCGTCATTTATG	TAGGTTGCATTTTCATCCTT
19	5'	CTCTGGTCGTTTCAGTG	TAGGTTGCATTTTCATCCTT
20	5'	CAGATGAGTGGAGCAA	TAGGTTGCATTTTCATCCTT
2	5'	GTTACTGGGTCAGGGA	TAGGTTGCATTTTCATCCTT
3	5'	CCCTCCATATACATTTT	TAGGTTGCATTTTCATCCTT
4	5'	GAGTCCCATTCACCAAC	TAGGTTGCATTTTCATCCTT
5	3'	ACGCACAAGACAAAGA	CTCCCACCCAGTTTCATAG
6	5'	CCCGCAAATCTCACGA	TAGGTTGCATTTTCATCCTT
7	5'	GTTTGACAGTGGTGTTG	TAGGTTGCATTTTCATCCTT
8	5'	TGTTGAGACAATAGGGT	TAGGTTGCATTTTCATCCTT
9	5'	TCATGAACAAGTGCTGT	TAGGTTGCATTTTCATCCTT
10	5'	GGAATAGATTGTCTTGG	TAGGTTGCATTTTCATCCTT
11	3'	GGCTCTCTGGGGCATC	CAGGGGCCTGGGGAATG
12	5'	TGTTTGAGAGGCAGAA	TAGGTTGCATTTTCATCCTT
13	5'	AGGTACTTGGTGGTGA	TAGGTTGCATTTTCATCCTT
21	5'	TGAGTATCAGTATCATT	TAGGTTGCATTTTCATCCTT

Figure S11. PERV junctions remain intact in the 100% PERV-inactivated cells. A) PCR detection of PERV junctions in the 100% PERV-inactivated cells. All PERVs are labeled as in Figure 2A. Junctions from 5' LTR are labeled in black whereas those from 3' LTRs are shown in red. **B) Primers used to detect PERV junctions.** These primers were designed using the PacBio sequencing data around the PERV regions in FFF3.

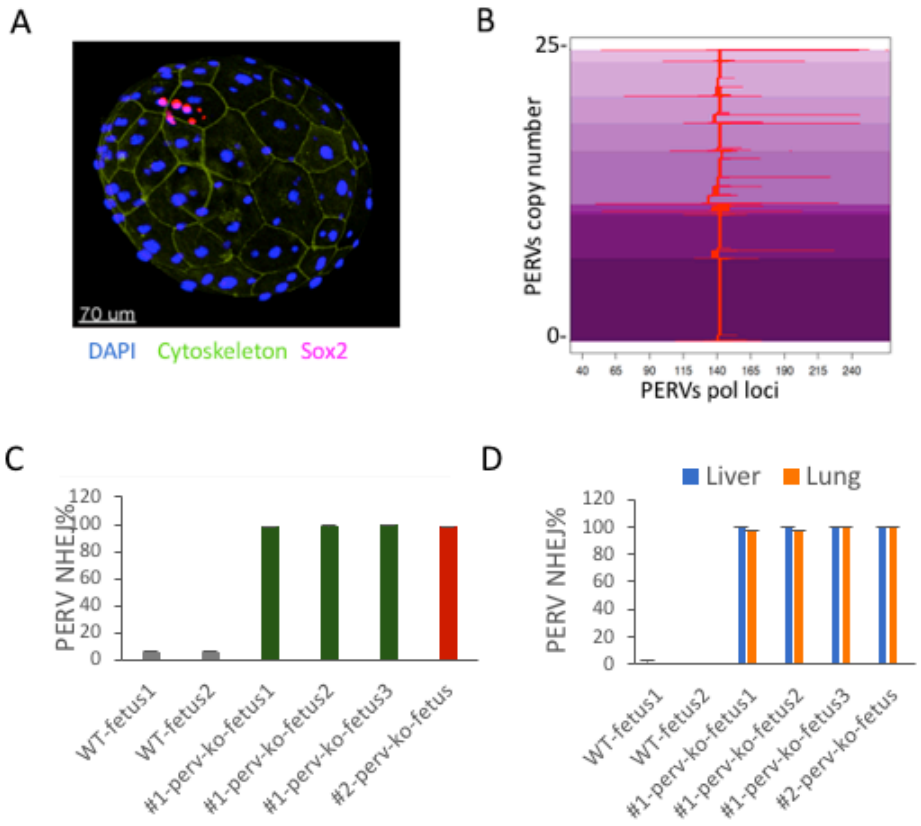

Figure S12. PERV-inactivated embryo and fetuses. A) Porcine blastocysts cloned from PERV-inactivated FFF3. Day 6 PERV-inactivated porcine blastocysts were stained with SOX2 (inner cell mass), DAPI (nuclei), and phalloidin (cell boundaries). Stained blastocysts were imaged using laser scanning confocal microscopy. **B) PERV targeting efficiency of embryo cloned from PERV-inactivated FFF3.** The y-axis indicates the edited PERVs loci. The x-axis indicates the relative locations of the indels within the PERV loci. Aligned indel events in the PERV *pol* sequence are represented in red. Shades of purple indicate different PERVs haplotypes. The genotype of the embryo showed that all the 25 copies of PERVs were successfully inactivated. **C) PERV-inactivation at genomic DNA level.** We genotyped PERV-inactivated and WT fetuses by deep sequencing of the PERV *pol* loci. All PERV-inactivated fetuses showed ~100% PERV inactivation. **D) PERV inactivation at mRNA level.** Total mRNA generated cDNA was used to detect the PERV inactivation efficiency of the PERV-inactivated fetuses in lung and liver. All PERV-inactivated fetuses exhibited ~100% PERV eradication efficiency at mRNA level.

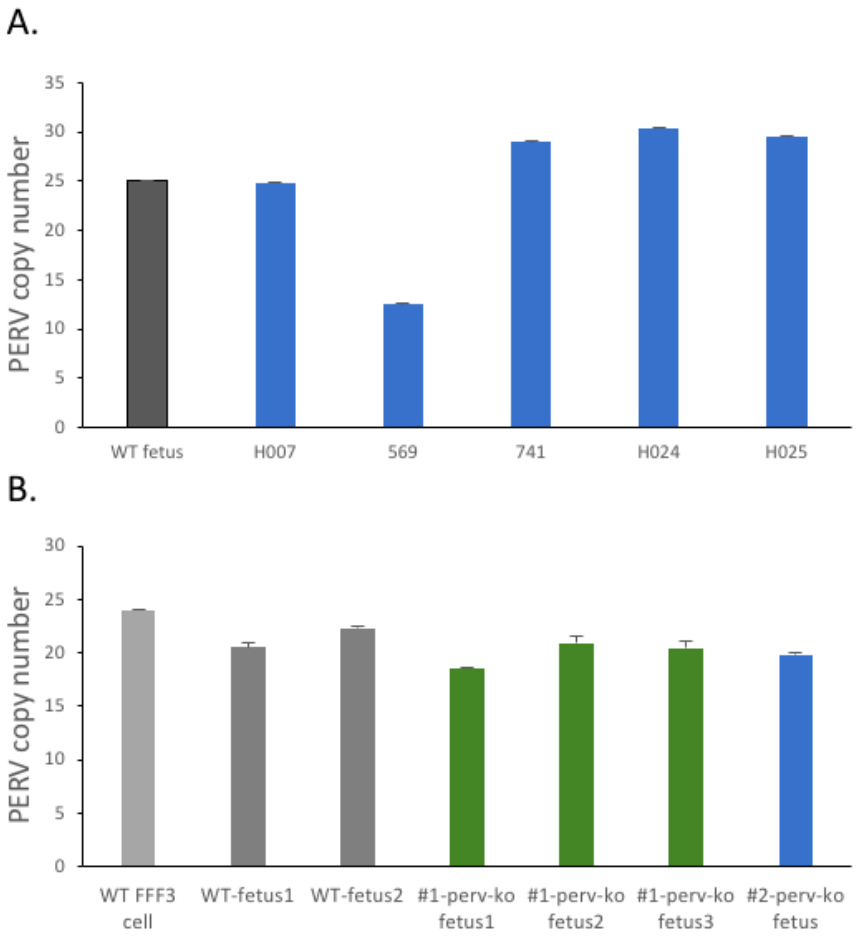

Figure S13. PERV copy number of surrogate sows and fetuses. A) PERV copy number of surrogate sows. Genomic DNAs of WT fetus and surrogate sows were used to measure PERV copy number by ddPCR. Different sows (H007, 569, 741, H024, H025) showed different PERV copy number (12~30). **B) PERV copy number of different fetuses.** Genomic DNAs of WT and PERV-inactivated fetuses and WT FFF3 fibroblast cells were used to measure PERV copy number by ddPCR. All fetuses showed similar PERV copy number as the WT FFF3 fibroblast cells.

Figure S14. Pictures of the newborn PERV-inactivated pigs (day 2-3) and 4-month old WT and PERV-inactivated pigs.

A

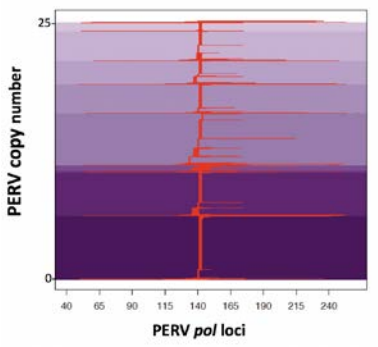

B

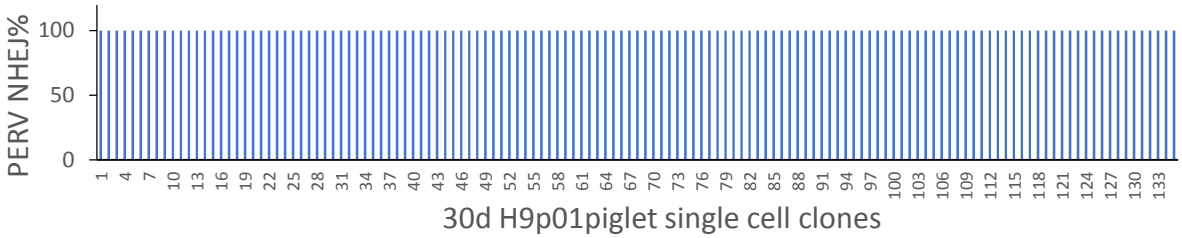

C

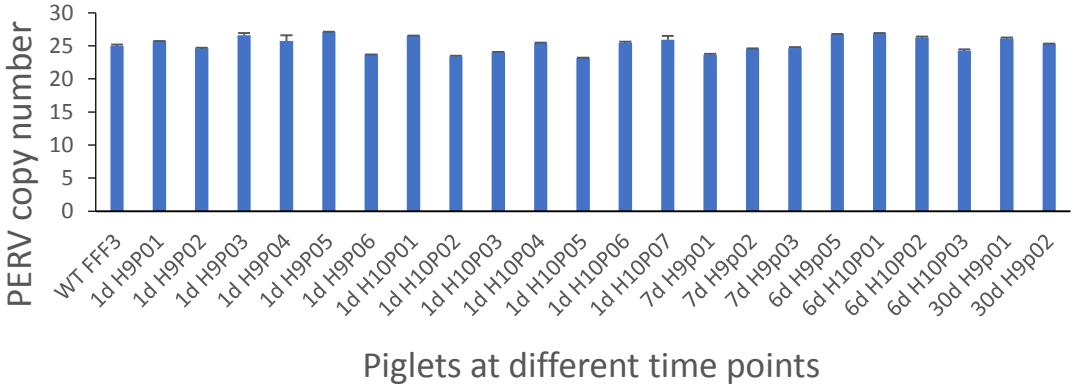

Fig. S15. Genotype of PERV-inactivated pigs. A) PERV targeting efficiency of a pig cloned from PERV-inactivated FFF3. The y-axis indicates the edited PERVs loci. The x-axis indicates the relative locations of the indels within the PERV loci. Aligned indel events in the PERV *pol* sequence are represented in red. Shades of purple indicate different PERVs haplotypes. The genotype of the piglet showed that all the 25 copies of PERVs were successfully inactivated. **B) PERV inactivation efficiency of single cells derived from a 30d PERV-inactivated pig.** Cells derived from a 30d H9p01 PERV-inactivated pig were sorted into single cells and PERV *pol* gene fragment were genotyped via deep sequencing using genomic DNA of the single cells as template. All single cells showed 100% PERV inactivation. **C) PERV copy number of PERV-inactivated pigs.** Genomic DNAs of PERV-inactivated pigs and WT FFF3 fibroblast cells were used to measure PERV copy number by ddPCR. All PERV-inactivated pigs showed similar PERV copy number as the WT FFF3 fibroblast cells.

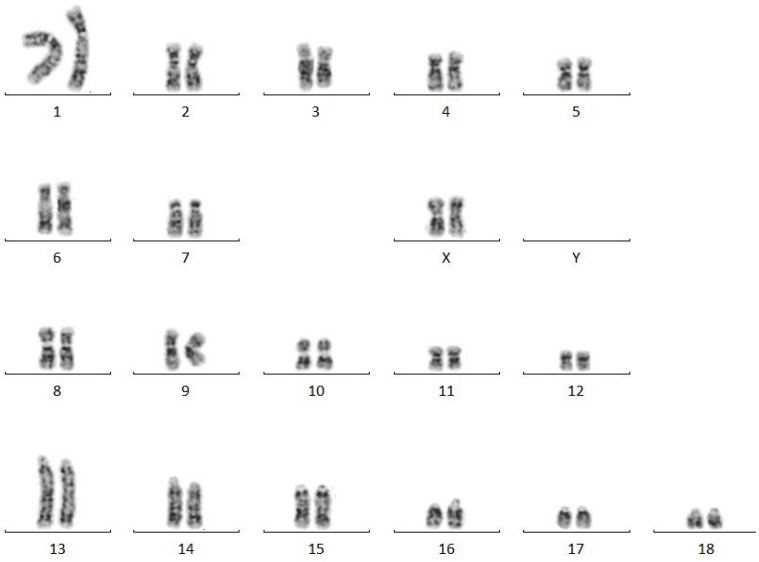

Fig. S16. Karyotyping of the cells from a PERV-inactivated pig. All PERV-inactivated pigs exhibited normal karyotype. We only present one of the karyotyping results here.

References and Notes

1. D. Shafran, E. Kodish, A. Tzakis, Organ shortage: The greatest challenge facing transplant medicine. *World J. Surg.* **38**, 1650–1657 (2014). doi:10.1007/s00268-014-2639-3 Medline

2. J.-Y. Deschamps, F. A. Roux, P. Saï, E. Gouin, History of xenotransplantation. *Xenotransplantation* **12**, 91–109 (2005). doi:10.1111/j.1399-3089.2004.00199.x Medline

3. C. Patience, Y. Takeuchi, R. A. Weiss, Infection of human cells by an endogenous retrovirus of pigs. *Nat. Med.* **3**, 282–286 (1997). doi:10.1038/nm0397-282 Medline

4. J. Denner, How active are porcine endogenous retroviruses (PERVs)? *Viruses* **8**, 215 (2016). doi:10.3390/v8080215 Medline

5. L. Yang, M. Güell, D. Niu, H. George, E. Lesha, D. Grishin, J. Aach, E. Shrock, W. Xu, J. Poci, R. Cortazio, R. A. Wilkinson, J. A. Fishman, G. Church, Genome-wide inactivation of porcine endogenous retroviruses (PERVs). *Science* **350**, 1101–1104 (2015). doi:10.1126/science.aad1191 Medline

6. Y. Moalic, Y. Blanchard, H. Félix, A. Jestin, Porcine endogenous retrovirus integration sites in the human genome: Features in common with those of murine leukemia virus. *J. Virol.* **80**, 10980–10988 (2006). doi:10.1128/JVI.00904-06 Medline

7. M. Bendinelli, D. Matteucci, H. Friedman, Retrovirus-induced acquired immunodeficiencies. *Adv. Cancer Res.* **45**, 125–181 (1985). doi:10.1016/S0065-230X(08)60268-7 Medline

8. L. J. Wegman-Points, M. L. T. Teoh-Fitzgerald, G. Mao, Y. Zhu, M. A. Fath, D. R. Spitz, F. E. Domann, Retroviral-infection increases tumorigenic potential of MDA-MB-231 breast carcinoma cells by expanding an aldehyde dehydrogenase (ALDH1) positive stem-cell like population. *Redox Biol.* **2**, 847–854 (2014). doi:10.1016/j.redox.2014.06.006 Medline

9. C. Patience, W. M. Switzer, Y. Takeuchi, D. J. Griffiths, M. E. Goward, W. Heneine, J. P. Stoye, R. A. Weiss, Multiple groups of novel retroviral genomes in pigs and related species. *J. Virol.* **75**, 2771–2775 (2001). doi:10.1128/JVI.75.6.2771-2775.2001 Medline

10. J. Zhao, J. Whyte, R. S. Prather, Effect of epigenetic regulation during swine embryogenesis and on cloning by nuclear transfer. *Cell Tissue Res.* **341**, 13–21 (2010). doi:10.1007/s00441-010-1000-x Medline

11. M. A. M. Groenen, A. L. Archibald, H. Uenishi, C. K. Tuggle, Y. Takeuchi, M. F. Rothschild, C. Rogel-Gaillard, C. Park, D. Milan, H.-J. Megens, S. Li, D. M. Larkin, H. Kim, L. A. F. Frantz, M. Caccamo, H. Ahn, B. L. Aken, A. Anselmo, C. Anthon, L. Auvil, B. Badaoui, C. W. Beattie, C. Bendixen, D. Berman, F. Blecha, J. Blomberg, L. Bolund, M. Bosse, S. Botti, Z. Bujie, M. Bystrom, B. Capitanu, D. Carvalho-Silva, P. Chardon, C. Chen, R. Cheng, S.-H. Choi, W. Chow, R. C. Clark, C. Clee, R. P. M. A. Crooijmans, H. D. Dawson, P. Dehais, F. De Sapio, B. Dibbits, N. Drou, Z.-Q. Du, K. Eversole, J. Fadista, S. Fairley, T. Faraut, G. J. Faulkner, K. E. Fowler, M. Fredholm, E. Fritz, J. G. R. Gilbert, E. Giuffra, J. Gorodkin, D. K. Griffin, J. L. Harrow, A. Hayward, K. Howe, Z.-L. Hu, S. J. Humphray, T. Hunt, H. Hornshøj, J.-T. Jeon, P. Jern, M. Jones, J. Jurka, H. Kanamori, R. Kapetanovic, J. Kim, J.-H. Kim, K.-W. Kim, T.-H. Kim, G.

Larson, K. Lee, K.-T. Lee, R. Leggett, H. A. Lewin, Y. Li, W. Liu, J. E. Loveland, Y. Lu, J. K. Lunney, J. Ma, O. Madsen, K. Mann, L. Matthews, S. McLaren, T. Morozumi, M. P. Murtaugh, J. Narayan, D. T. Nguyen, P. Ni, S.-J. Oh, S. Onteru, F. Panitz, E.-W. Park, H.-S. Park, G. Pascal, Y. Paudel, M. Perez-Enciso, R. Ramirez-Gonzalez, J. M. Reecy, S. Rodriguez-Zas, G. A. Rohrer, L. Rund, Y. Sang, K. Schachtschneider, J. G. Schraiber, J. Schwartz, L. Scobie, C. Scott, S. Searle, B. Servin, B. R. Southey, G. Sperber, P. Stadler, J. V. Sweedler, H. Tafer, B. Thomsen, R. Wali, J. Wang, J. Wang, S. White, X. Xu, M. Yerle, G. Zhang, J. Zhang, J. Zhang, S. Zhao, J. Rogers, C. Churcher, L. B. Schook, Analyses of pig genomes provide insight into porcine demography and evolution. *Nature* **491**, 393–398 (2012). doi:10.1038/nature11622 Medline

12. M. Güell, L. Yang, G. M. Church, Genome editing assessment using CRISPR Genome Analyzer (CRISPR-GA). *Bioinformatics* **30**, 2968–2970 (2014). doi:10.1093/bioinformatics/btu427 Medline

13. J. Zhang, K. Kobert, T. Flouri, A. Stamatakis, PEAR: A fast and accurate Illumina Paired-End reAd mergeR. *Bioinformatics* **30**, 614–620 (2014). doi:10.1093/bioinformatics/btt593 Medline

14. R. Tomii, M. Kurome, N. Wako, T. Ochiai, H. Matsunari, K. Kano, H. Nagashima, Production of cloned pigs by nuclear transfer of preadipocytes following cell cycle synchronization by differentiation induction. *J. Reprod. Dev.* **55**, 121–127 (2009). doi:10.1262/jrd.20126 Medline

15. H. Wei, Y. Qing, W. Pan, H. Zhao, H. Li, W. Cheng, L. Zhao, C. Xu, H. Li, S. Li, L. Ye, T. Wei, X. Li, G. Fu, W. Li, J. Xin, Y. Zeng, Comparison of the efficiency of Banna miniature inbred pig somatic cell nuclear transfer among different donor cells. *PLOS ONE* **8**, e57728 (2013). doi:10.1371/journal.pone.0057728 Medline